Particle attenuation within dark matter spikes

Mainly based on JCAP 05 (2023) 057 and 2307.09460

Gonzalo Herrera
gonzaloherrera@vt.edu

Virginia Tech Center for Neutrino Physics
Technische Universität München
Max Planck Institute for Physics

In collaboration with Alejandro Ibarra, Francesc Ferrer, Kohta Murase and Elisa Resconi

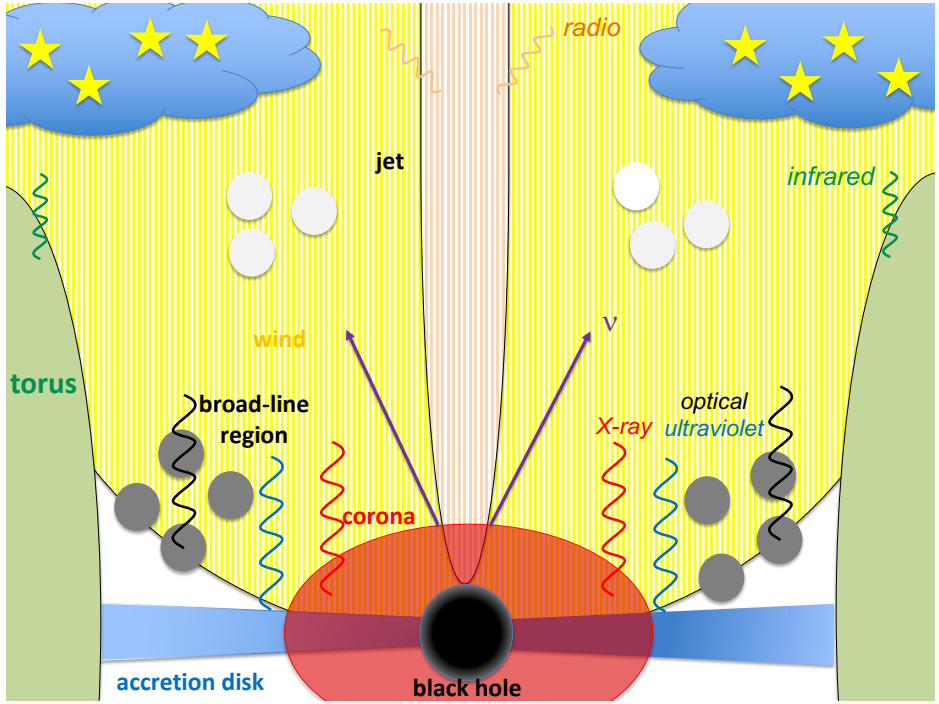

In an Active Galactic Nucleus (AGN), the emitted neutrino flux is proportional to the injected proton flux from the accretion disk (**Berezinsky, 77'**)

- $p + \gamma \longrightarrow n + \pi^+$
  $\pi^+ \longrightarrow e^+ + \nu_\mu + \nu_e$

  $p + \gamma \longrightarrow p + \pi^0$
  $\pi^0 \longrightarrow \gamma + \gamma$

Both processes occur with similar probability:

Comparable neutrino and gamma-ray fluxes!

High-energy multi-messenger astronomy

- Photons: Extragalactic sources of high-energy gamma-rays have been identified for several years (e.g AGN, Gamma-ray bursts, Starbust galaxies)
- Neutrinos: Not long ago, the only well known astrophysical sources were the Sun and Supernova 1987A, whereas the origin of the diffuse flux of high-energy cosmic neutrinos remained unclear.

IceCube, 13'

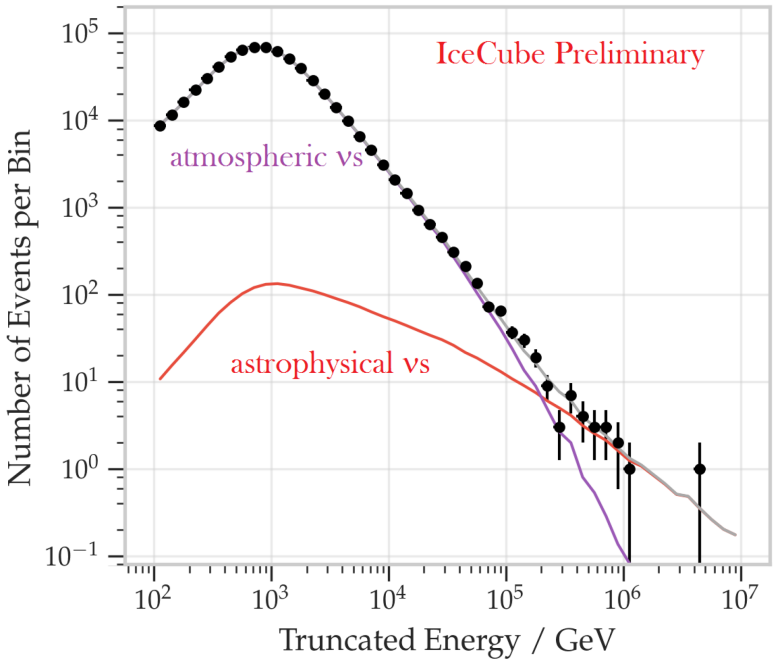

Fermi LAT, 14'

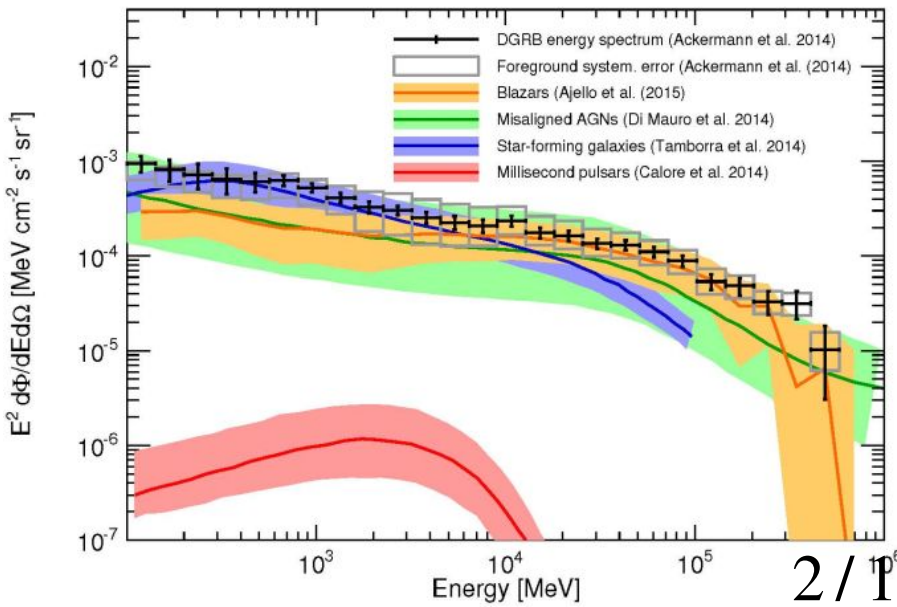

Astrophysical neutrino sources

Oikonomou, 22'

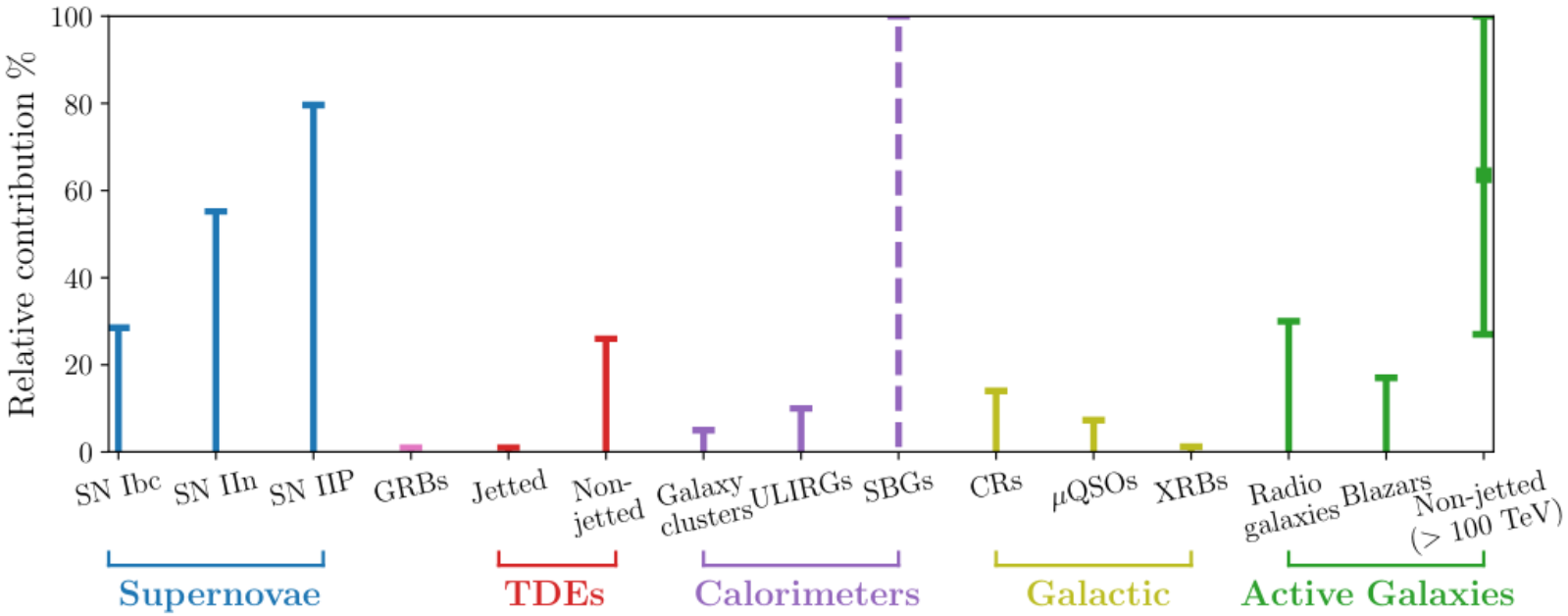

- Blazars: A $\sim$ 290 TeV muon neutrino, identified with the blazar TXS 0506+056 in flaring state. Subsequent analysis by IceCube with 9.5 yr data found additional $\sim$ 13 events at 3.5 σ.
- Non-jetted active galaxies: IceCube observed $\sim$ 80 neutrinos from the galaxy NGC 1068, at 4.2 σ.
- Tidal disruption events (TDEs): Hints of three events (AT2019dsg, AT2019fdr, AT2019aalc) at 3.7 σ suggested by independent groups.

Emitting region in TXS 0506+056

Gao, Fedynitch, Winter, Pohl, 19'

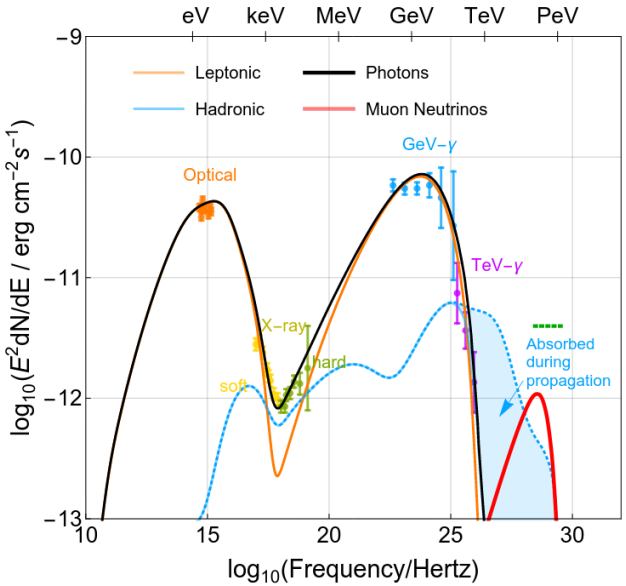

Padovani, Oikonomou, Petropoulou, Giommi, Resconi, 19'

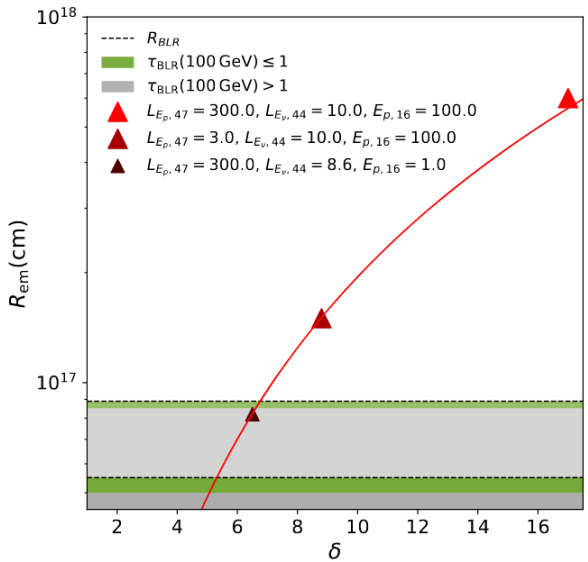

- Single-zone leptohadronic models can accommodate observations to some significance

- The emitting region is likely to be located near, or beyond the Broad Line Region (BLR), $R_{em} \approx R_{BLR} \approx 0.023$ pc

- An emitting region closer to the black hole is disfavoured, since stronger internal absorption of ~ 100 GeV gamma-rays by the BLR would have been expected.

Flux attenuation from TXS 0506+056 to the Earth

- Gamma-rays and neutrinos are subject to attenuation during propagation to the Earth due to SM processes.
- They may also be attenuated due to scatterings with dark matter particles on their path to the Earth.

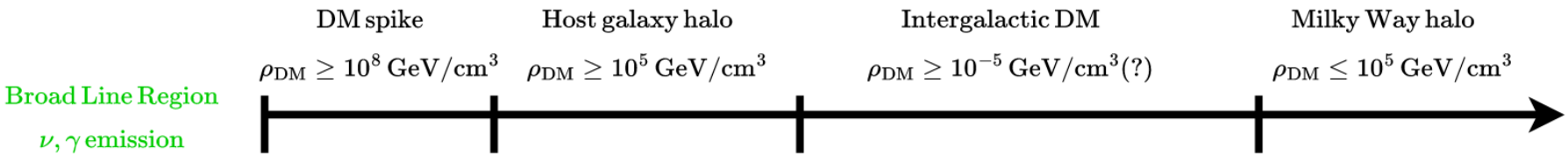

- Previous works considered solely the attenuation of neutrinos in the intergalactic medium and Milky Way halo

  Argüelles, Kheirandish, Vincent 17'
  Choi, Kim, Rott 19'

- However, the dark matter density in the vicinity of TXS 0506+056 is expected to be significantly larger

Dark matter spike formation

Adiabatic growth: A substantial increase in $M_{\rm BH}$ takes place after its initial formation, and the mass is acretted slowly to the pre-existing seed.

Peebles, 72'
Quinlan, Hernquist, Sigurdsson, 95'

Adiabatic conditions :

$f'(E', L') = f(E, L) \rightarrow$ Phase-space distribution conservation

$L' = L \rightarrow$ Angular momentum conservation

$I'(E', L') = I(E, L) \rightarrow$ Radial action conservation

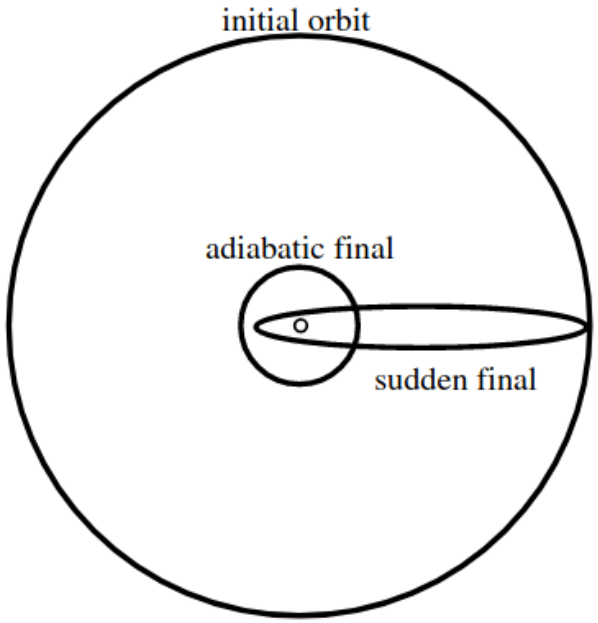

Ullio, Zhao, Kamionkowski, 01'

The dark matter spike profile

The dark matter in the vicinity of a black hole that grows adiabatically forms a dense spike with profile:

Gondolo, Silk, 99'

$$\rho_{\rm sp}(r) = \rho_R \, g_\gamma(r) \left(\frac{R_{\rm sp}}{r}\right)^{\gamma_{\rm sp}}$$

- $\rho_R = \rho_0 \left(R_{\rm sp}/r_0\right)^{-\gamma}$

  Normalization factor

- $R_{\rm sp} = \alpha_\gamma r_0 \left(M_{\rm BH}/(\rho_0 r_0^3)\right)^{\frac{1}{3-\gamma}}$

  Size of the spike

- $\gamma_{\rm sp} = \frac{9-2\gamma}{4-\gamma}$

  Cuspiness of the spike

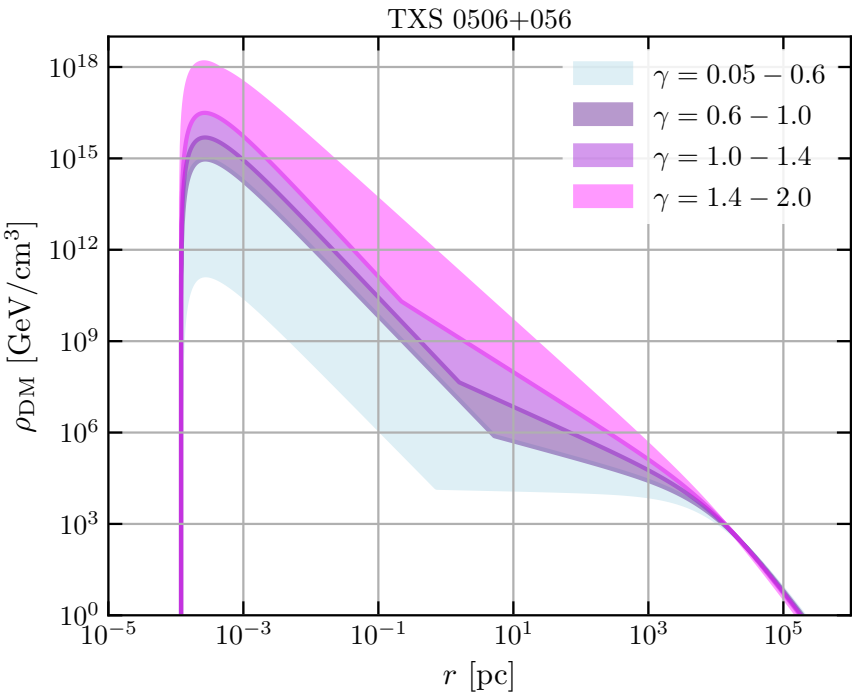

Only valid for $r \leq R_{\rm sp}$, and in scenarios where the dark matter does not self-annihilate (e.g asymmetric dark matter or axions).

The dark matter profile around TXS 0506+056

When the dark matter particles annihilate, the maximal density in the spike is saturated

- $\frac{dn_{\rm DM}(t,r)}{dt} = \langle\sigma v\rangle n^2_{\rm DM}(t,r) \rightarrow n_{\rm DM}(t,r) \simeq \frac{n_{\rm DM}(t_f,r)}{1+n_{\rm DM}(t_f,r)\langle\sigma v\rangle(t-t_f)}$

$$\rho_{\rm sat} = m_{\rm DM}/(\langle\sigma v\rangle t_{\rm BH})$$

- $t_{\rm BH} \rightarrow$ Time elapsed since the black hole formation.
- $\langle\sigma v\rangle \rightarrow$ Velocity averaged dark matter annihilation cross section.

$$\rho(r) = \begin{cases} 0 & r \leq 4R_S \\ \frac{\rho_{\rm sp}(r)\rho_{\rm sat}}{\rho_{\rm sp}(r)+\rho_{\rm sat}} & 4R_S \leq r \leq R_{\rm sp} \\ \rho_0 \left(\frac{r}{r_0}\right)^{-\gamma} \left(1+\frac{r}{r_0}\right)^{-(3-\gamma)} & r \geq R_{\rm sp}. \end{cases}$$

- With relativistic effects and/or rotating BH's, the spike vanishes at $2R_S$ and the density of DM particles is enhanced near the core (**Sadeghian, Ferrer, Will, 13'** **Ferrer, Medeiros da Rosa, Will, 17'**).

However, these effects do not change the profile in the region of the jet where neutrinos and gamma-rays are produced.

The dark matter profile around TXS 0506+056

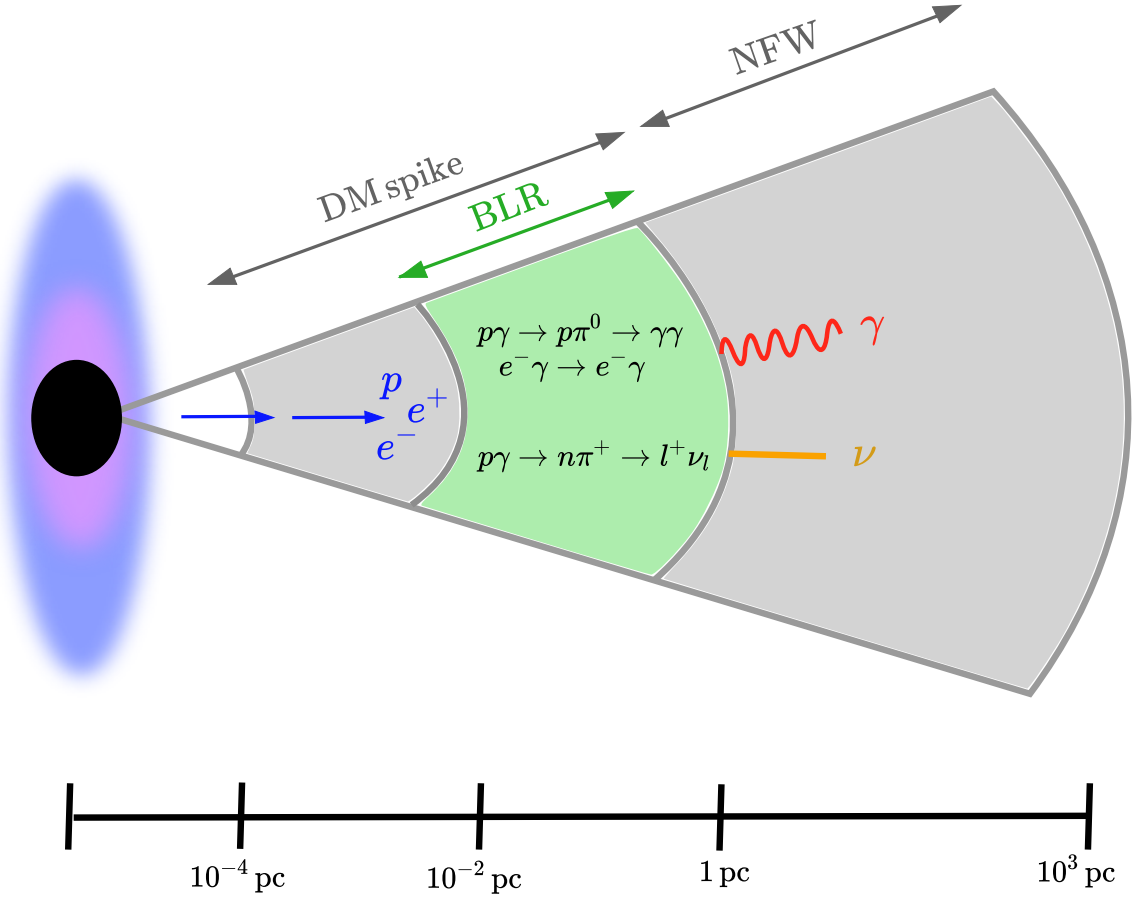

✓ High-energy neutrinos and gamma-rays are likely to be produced within the dark matter spike of TXS 0506+056.

The dark matter profile around TXS 0506+056

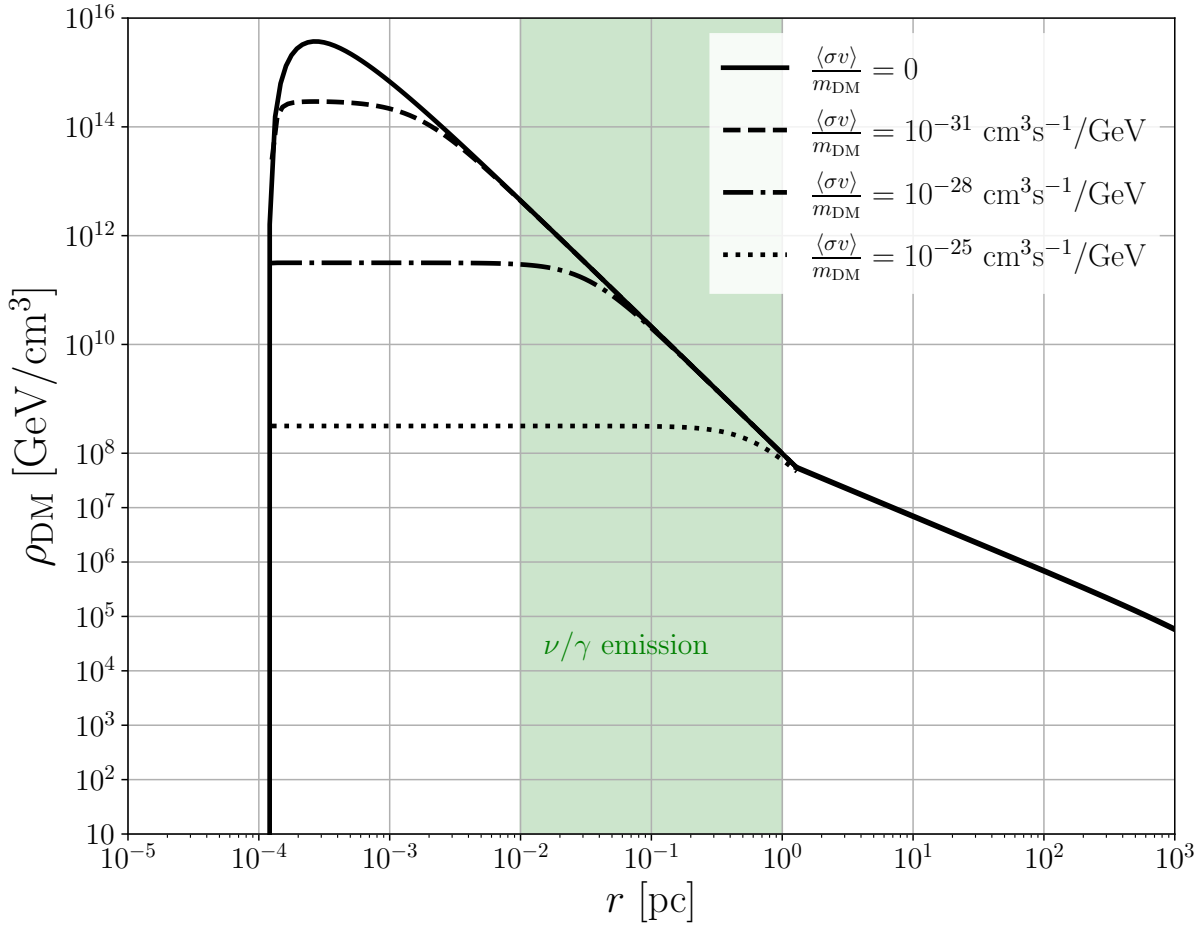

✓ High-energy neutrinos and gamma-rays are likely to be produced within the dark matter spike of TXS 0506+056.

A criteria for the flux atttenuation

The attenuation of the neutrino and photon fluxes produced at the distance $R_{\rm em}$ from the BH can be described by

$$\frac{d\Phi}{d\tau}(E_i) = -\sigma_{\rm DM-i}\Phi_i + \int_{E_\nu}^{\infty} dE_i' \frac{d\sigma}{dE_i}(E_i' \to E_i)\Phi(E_i')$$

with $\tau = \Sigma_{\rm DM}/m_{\rm DM}$

- Our criteria assumes implicitely that that emitted flux is larger than the observed flux, and the second term of the cascade equation can be neglected.
- $\Sigma_{\rm DM} \simeq \int_{\rm path} dr\rho(r) \simeq \int_{R_{\rm em}}^{R_{\rm sp}} dr\rho(r) + \int_{R_{\rm sp}}^{\infty} dr\rho(r)$

Imposing that the attenuation of the neutrino flux due to DM-neutrino scatterings is less than 90%, and less than 99% for DM-photon scatterings

$$\frac{\sigma_{\rm DM-\nu}}{m_{\rm DM}} \lesssim \frac{2.3}{\Sigma_{\rm DM}} \quad , \frac{\sigma_{\rm DM-\gamma}}{m_{\rm DM}} \lesssim \frac{4.6}{\Sigma_{\rm DM}}$$

The dark matter column density around TXS 0506+056

The column density on the spike from $R_{\rm em}$ reads

$$\text{Small } \langle\sigma v\rangle \rightarrow \quad \Sigma_{\rm DM}\Big|_{\rm spike} \simeq \frac{\rho_{\rm sp}(R_{\rm em})R_{\rm em}}{(\gamma_{\rm sp}-1)}\left[1-\left(\frac{R_{\rm sp}}{R_{\rm em}}\right)^{1-\gamma_{\rm sp}}\right]$$

$$\text{Large } \langle\sigma v\rangle \rightarrow \quad \Sigma_{\rm DM}\Big|_{\rm spike} \simeq \rho_{\rm sat}R_{\rm sp}\left[1-\frac{R_{\rm em}}{R_{\rm sp}}\right] \propto m_{\rm DM}/\langle\sigma v\rangle$$

And the contribution from the the halo of the host galaxy reads

$$\Sigma_{\rm DM}\Big|_{\rm host} \simeq \rho_0 r_0\left[\log\left(\frac{r_0}{R_{\rm sp}}\right)-1\right]$$

In general not negligible when compared to the contribution from the spike

Ferrer, Herrera, Ibarra, 22'

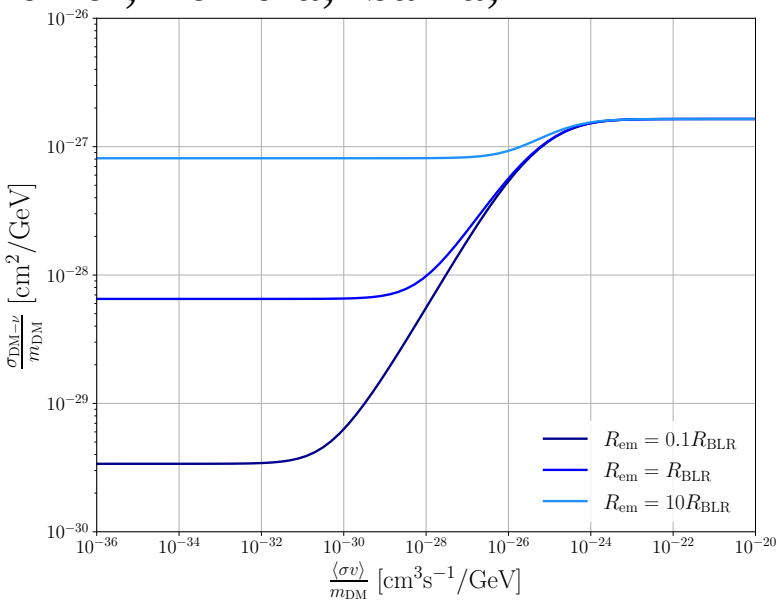

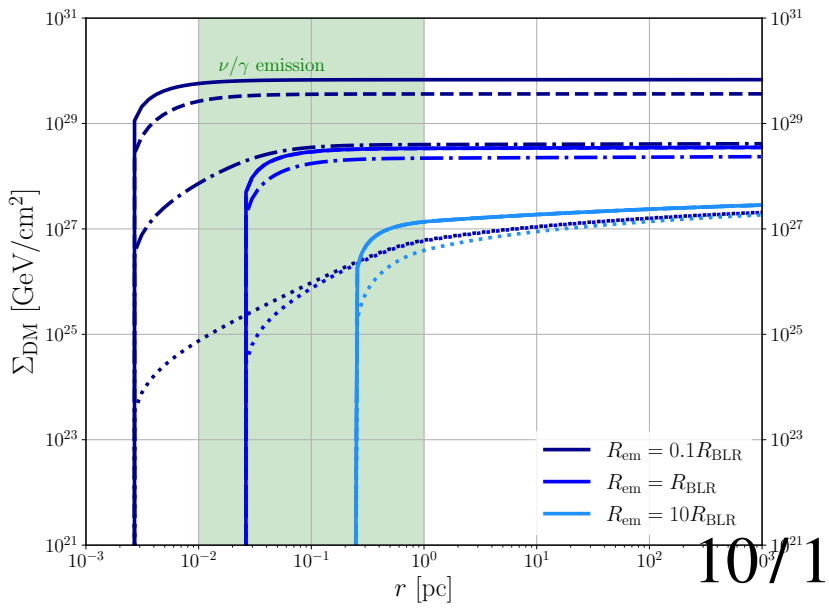

Constraints on the constant DM-ν cross section

Ferrer, Herrera, Ibarra, 22'
Cline et al, 22'

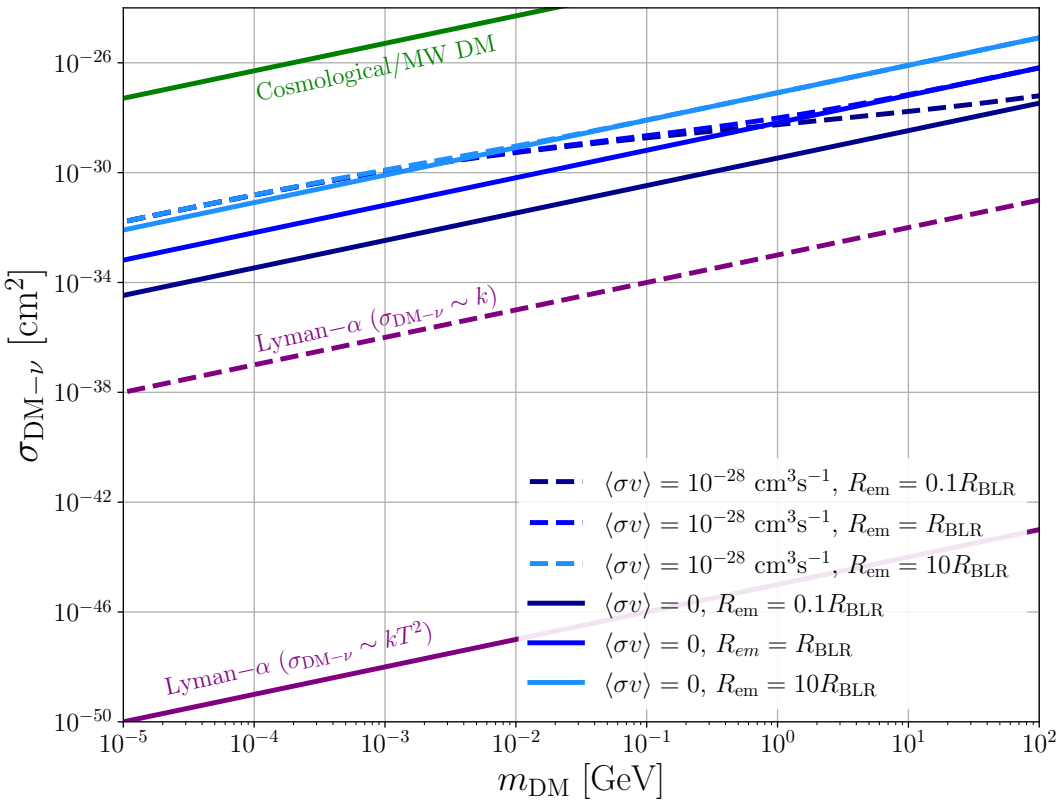

- The constraints are ~ 5 orders of magnitude stronger than those obtained from the intergalactic medium and the MW.
- The constraints are ~ 5 orders of magnitude weaker than the constraints from the Lyman-α forest

Constraints on the constant DM-γ cross section

Ferrer, Herrera, Ibarra, 22'

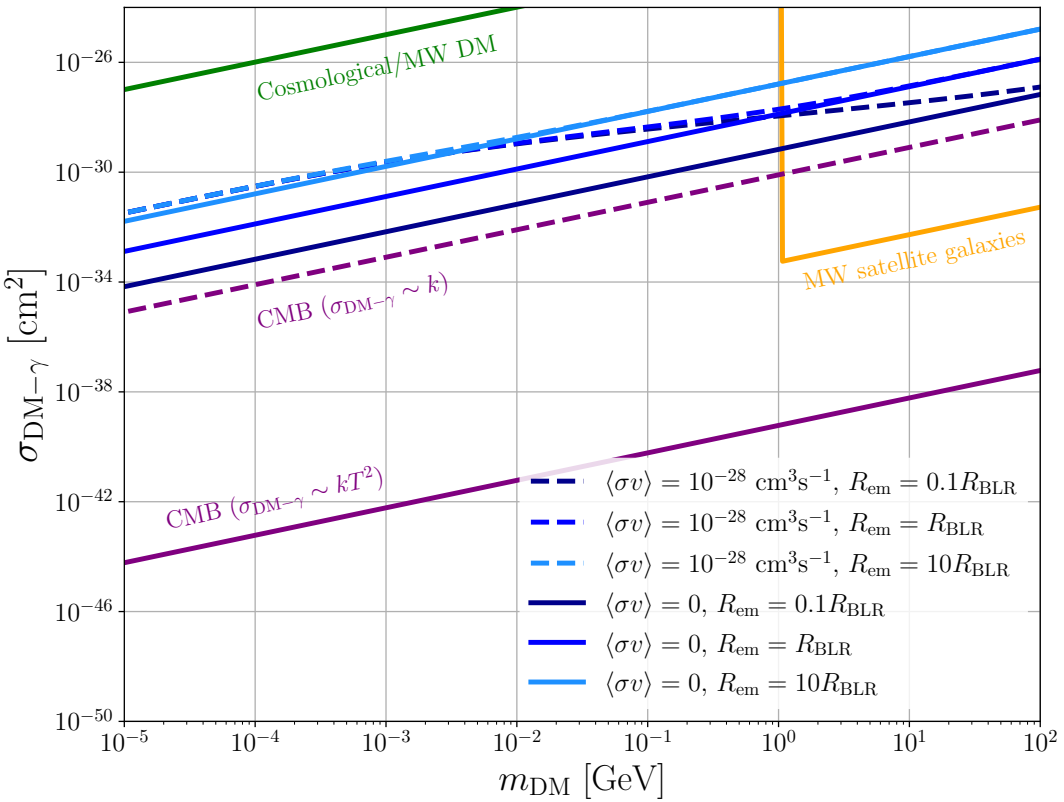

- The constraints are ~ 5 orders of magnitude stronger than those obtained from the intergalactic medium and the MW.
- The constraints are ~ 2 orders of magnitude weaker than the constraints from the CMB and MW satellite galaxy counts.

Constraints on energy-dependent cross sections

In any realistic model, the DM-neutrino and DM-photon scattering cross sections will depend non-trivially on the incoming particle energy, e.g:

- Fermion DM-neutrino scattering via a Z' mediator $\rightarrow \sigma_{\mathrm{DM}-\nu} \propto E_\nu$.
- Scalar DM-neutrino scattering via a fermion mediator $\rightarrow \sigma_{\mathrm{DM}-\nu} \propto E_\nu^2$
- Fermion DM-photon scattering via higher dimension ≥ 5 operators $\rightarrow \sigma_{\mathrm{DM}-\gamma} \propto E_\gamma^2$ or E_γ^4 .

A proper comparison between upper limits requires a rescaling for the energy at which every limit applies.

Constraints on energy-dependent cross sections

Ferrer, Herrera, Ibarra, 22'

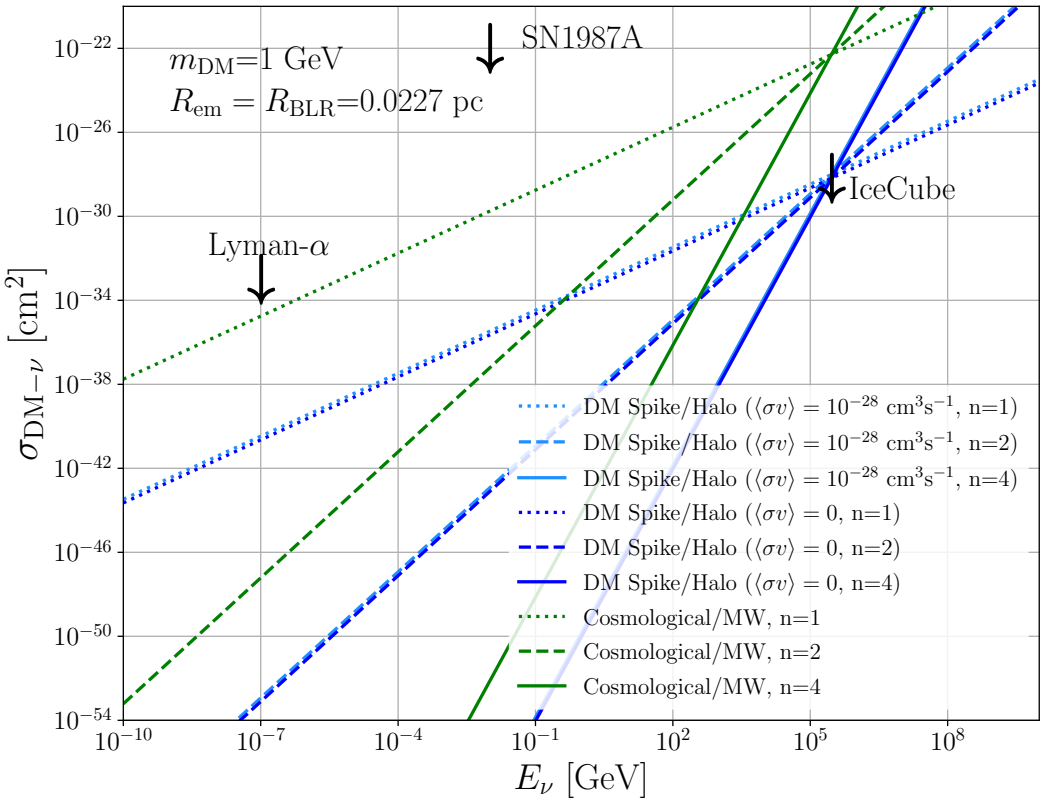

- If the cross section scales linearly with the energy of the neutrino, our constraints are ~ 7 orders of magnitude stronger than those from cosmology.

Constraints on energy-dependent cross sections

Ferrer, Herrera, Ibarra, 22'

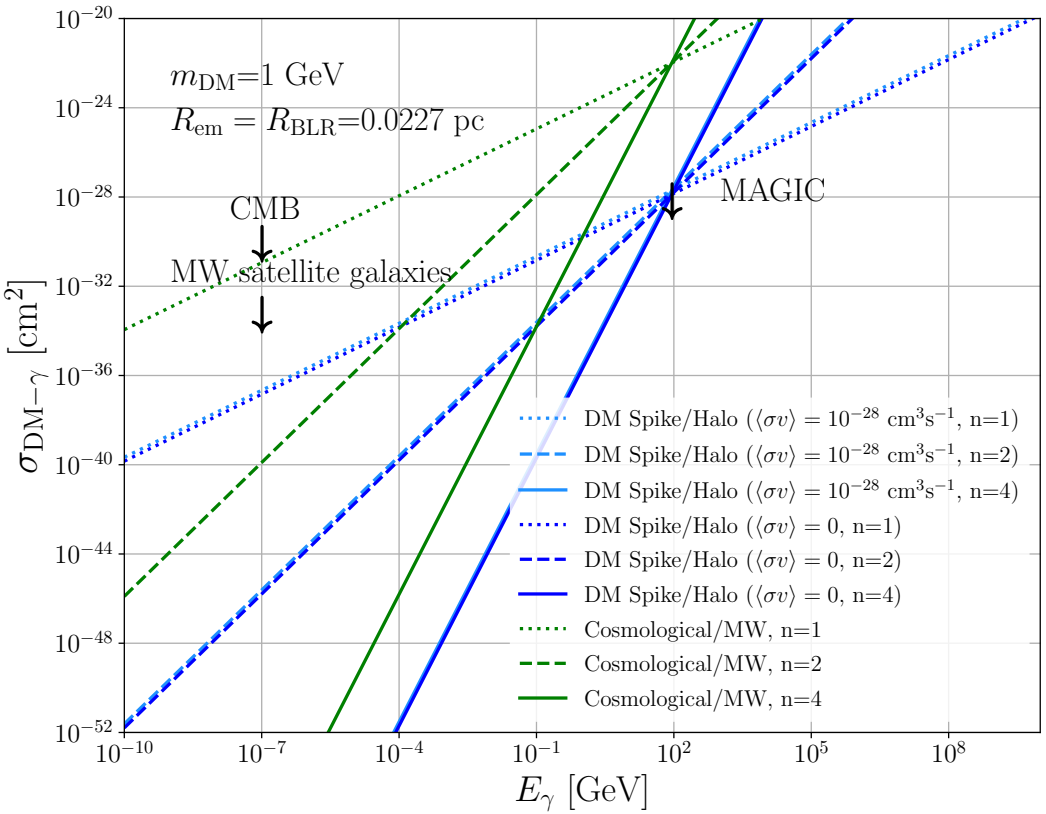

- If the cross section scales linearly with the energy of the neutrino, our constraints are ~ 4 orders of magnitude stronger than those from cosmology.

A hint of dark matter-photon scattering in NGC 1068

$$\Delta\mu(E_\gamma) \simeq \left(\frac{M_{\rm BH}}{2\times10^7 M_\odot}\right)^{3/4}\left(\frac{r_0}{10\,{\rm kpc}}\right)^{1/2}\left(\frac{\rho_0}{0.043 M_\odot/{\rm pc}^3}\right)^{3/8}\left(\frac{R_{\rm em}}{10^3 R_{\rm S}}\right)^{-11/8}\left(\frac{m_{\rm DM}}{1\,{\rm GeV}}\right)^{-1}\left(\frac{\sigma_{{\rm DM}-\gamma}(E_\gamma)}{10^{-29}\,{\rm cm}^2}\right)$$

- O(1) absorption requires cross sections of $\sim 10^{-29}{\rm cm}^2$
- In some particle physics models, these values might be achieved via the inelastic scattering DM + $\gamma \rightarrow$ DM+X, where X is a scalar/pseudoscalar/vector.

Herrera, Ibarra, Resconi, *In progress*

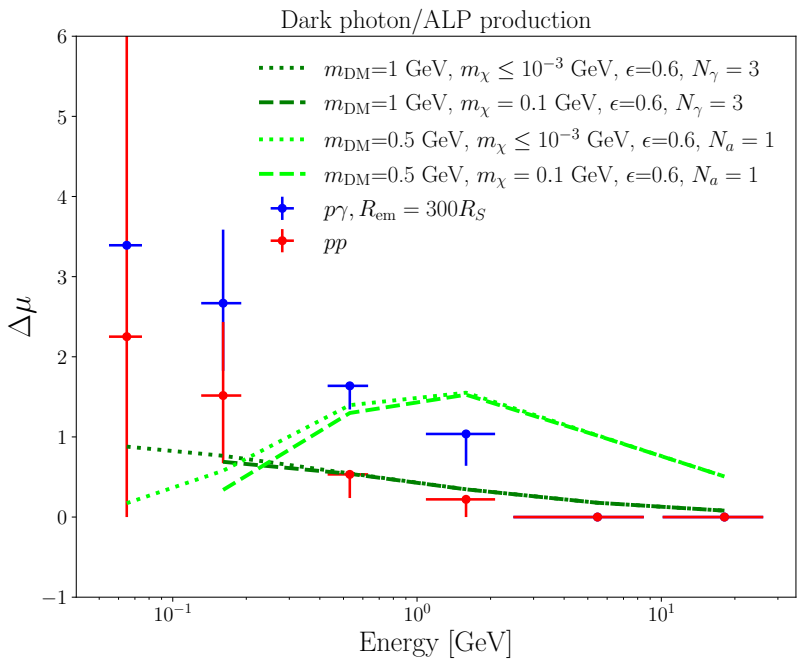

Minimal scenarios can't induce observable attenuations, but dark sectors with a few extra parameters can do the job.

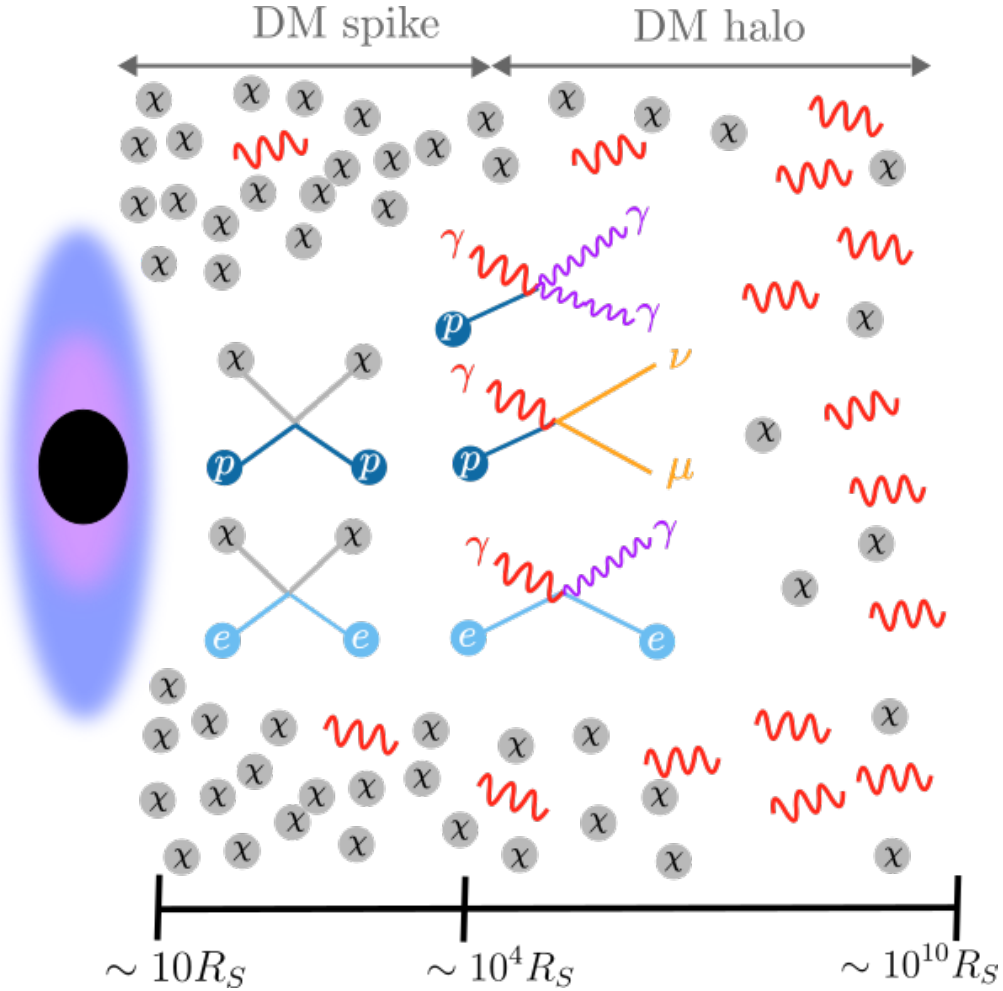

- High-energy protons and electrons can cool efficiently via interactions with ambient photons and gas in the AGN

- May they also cool via scatterings with the ambient dark matter particles ?

Cosmic ray cooling in the dark matter spike

Simple estimate → The currently strongest bound on light dark matter coupling to protons is given by the direct detection of cosmic-ray boosted dark matter

E.g for $m_{\rm DM} \sim 10^{-3}$ GeV $\rightarrow \sigma_{\rm DM-p} \lesssim 10^{-35}$ cm^2

The average dark matter spike density in the corona of NGC 1068 is

$$\langle \rho_{\rm DM} \rangle \sim 5 \times 10^{18} {\rm GeV/cm^3} \text{ for } \gamma = 1.$$

$$\tau_{{\rm DM}-p} \sim 1/\left(\langle n_{\rm DM} \rangle \, \sigma_{{\rm DM}-p} c\right) \sim 7 \times 10^3 \text{ s}$$

This value is well below the proton cooling timescale inferred by observations of NGC 1068 ($\sim 10^6$s).

Cosmic rays in AGN can provide a powerful probe of light dark matter !

Cosmic ray cooling in the dark matter spike

We find for each $m_{\rm DM}$ the largest DM-proton (electron) cross section yielding a timescale equal or larger to the cooling timescales determined with models at the relevant energies ($\tau^{\rm el}_{{\rm DM}-i} \geq C\tau^{\rm cool}_i$, with $C \sim 0.1-1$)

$$\tau^{\rm el}_{{\rm DM}-i} = \left[-\frac{1}{E}\left(\frac{dE}{dt}\right)_{{\rm DM}-i} \right]^{-1}$$

$$\left(\frac{dE}{dt}\right)_{{\rm DM}-i} = \frac{\rho_{\rm DM}}{m_{\rm DM}} \int_0^{T^{\rm max}_{\rm DM}} dT_{\rm DM}\, T_{\rm DM} \frac{d\sigma_{\rm el}}{dT_{\rm DM}}$$

Herrera, Murase, 23'

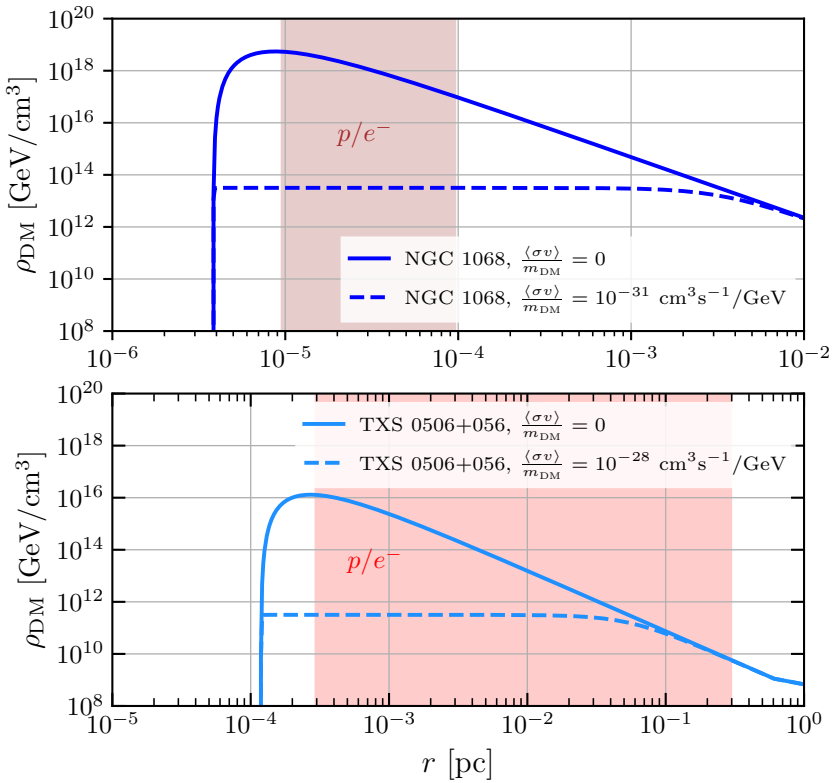

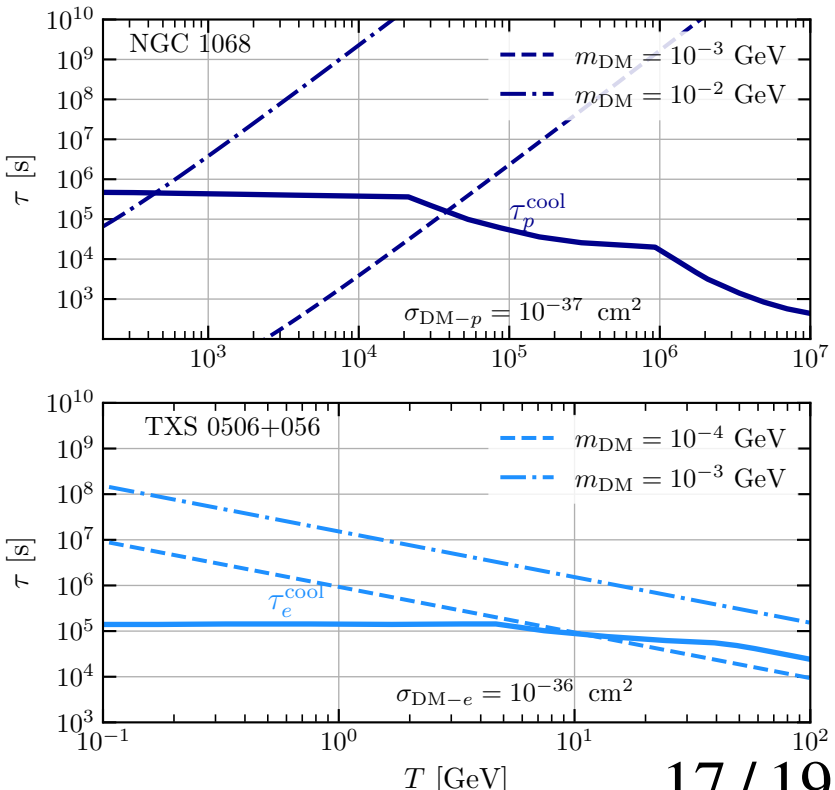

Cosmic ray cooling in the dark matter spike

Herrera, Murase, 23'

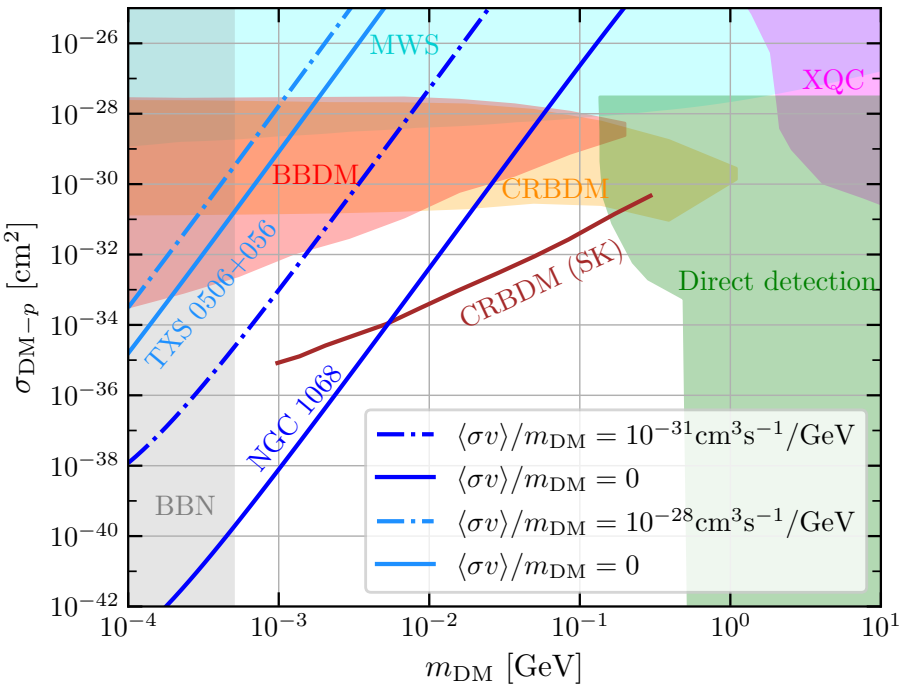

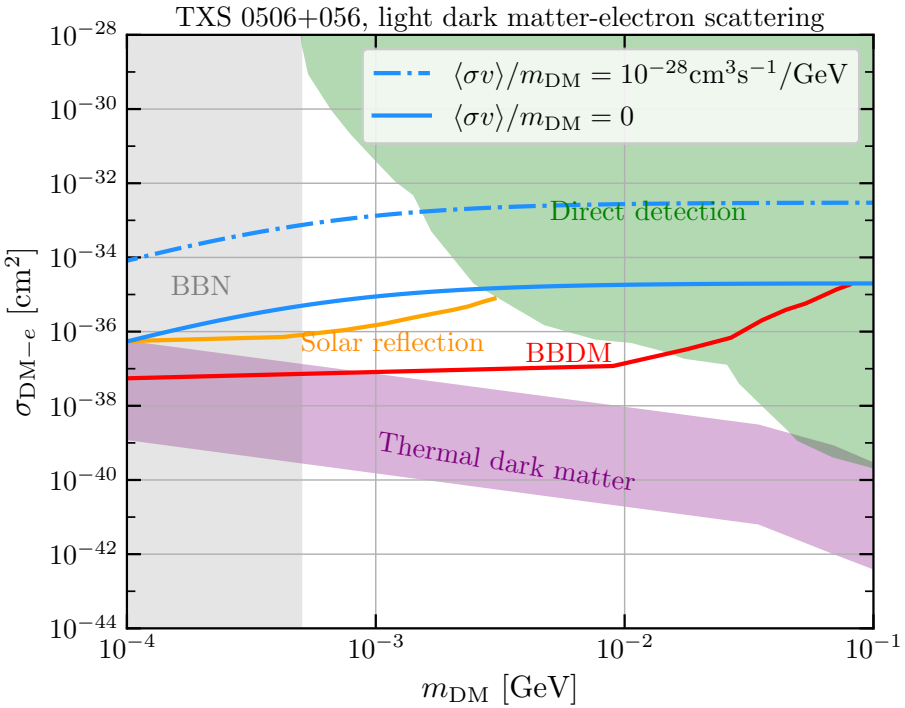

- Strongest constraint to date on light dark matter coupling to protons for $m_{\rm DM} \lesssim 10^{-3} - 10^{-2}$ GeV.

- Strongest bound on light dark matter coupling to electrons for $m_{\rm DM} \lesssim 10^{-4}$ GeV.

Conclusions

- **Standard model particles may scatter off dark matter particles in AGN, being their fluxes attenuated**

- We find constraints for DM-ν and DM-γ scatterings which are orders of magnitude stronger than those obtained from the attenuation in the intergalactic medium and the Milky Way, and stronger than cosmological ones in some models.

- We have proposed cosmic-ray cooling in AGN as a new probe of dark matter scatterings with protons and electrons, finding strong constraints on the parameter space of light dark matter.

- Our results are subject to uncertainties from the proton and electron luminosities, from the emitting region of neutrinos and gamma-rays, and from the dark matter profile.

Thanks for your attention

gonzaloherrera@vt.edu

Constraints on DM spike in the MW

Constraints on the spike radius of the milky way vs NFW index γ, from the astrometric and spectroscopic data on the S2 star at the Galactic Centre

Gravitational scatterings of stars and dark matter may relax the dark matter spike to $\gamma_{sp} = 1.5$, due to both kinetic heating and capture.

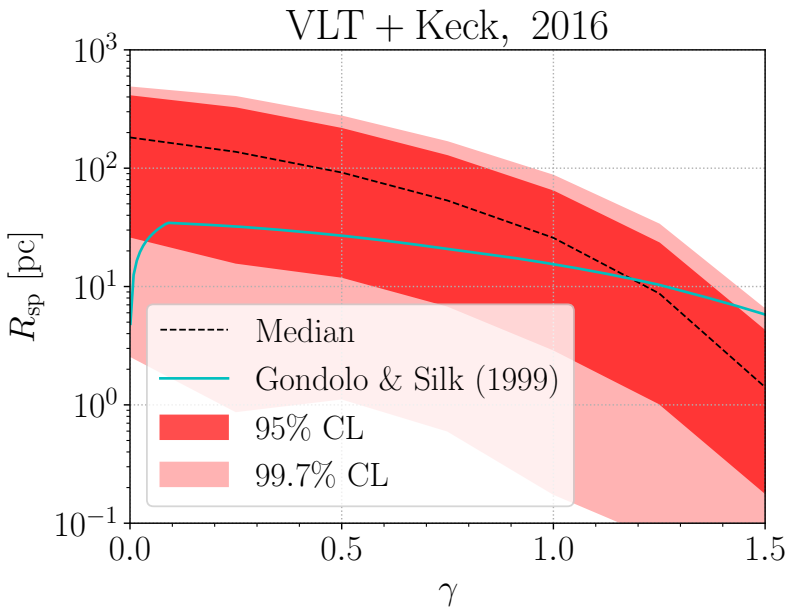

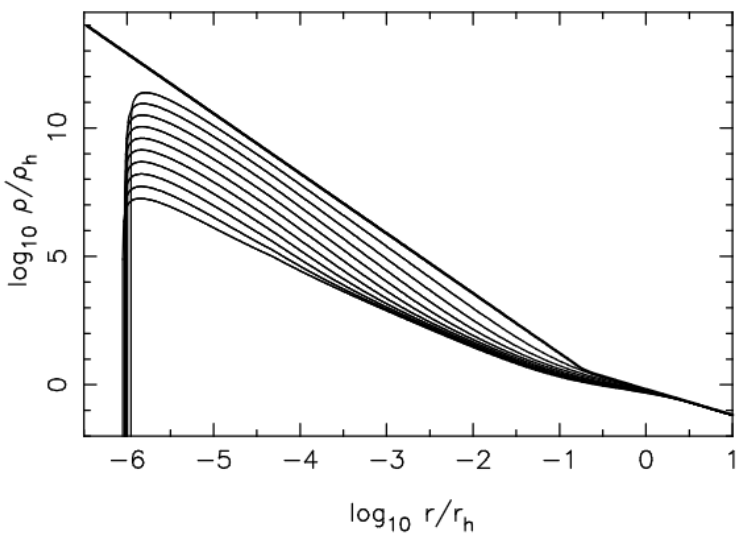

Lacroix, 18'
Merrit, 04'

Adiabatic growth condition

Adiabatic growth motivated for DM due to collisionless nature

Satisfied if the timescale for BH growth due to accretion of both baryonic and DM is longer than the dynamical timescale of DM and baryons in the radius of black hole dominance, $r_h = GM_{\rm BH}/\sigma^2$

The shortest BH growth timescale is given by the Salpeter timescale, $t_S \sim M_{\rm BH}/\dot{M}_{\rm Edd} \sim 5 \times 10^7$ yr, where $\dot{M}_{\rm Edd}$ is the Eddington accretion timescale.

The dynamical timescale is $t_{\rm dyn} = r_h/\sigma$. Our current knowledge on the relation between BH masses and velocity dispersion points towards the adiabatic growth regime for $M_{\rm BH} \lesssim 10^{10} M_\odot$.

Normalization of the spike

- For NFW with $\gamma = 1$, we follow criteria from Gorchtein et al: The DM spike in the region of BH dominance must agree with the uncertainty in the determination of the BH mass

$$\int_{4R_S}^{10^5 R_S} 4\pi r^2 \rho(r) \mathrm{d}r = \Delta M_{\mathrm{BH}}$$

  Assuming further that the mass is dominated by the contribution from $r > R_{\mathrm{min}} = O\left(100 R_S\right)$

$$\rho_0 = \left(\frac{\left(3 - \gamma_{\mathrm{sp}}\right) \Delta M_{\mathrm{BH}}}{4\pi R_{\mathrm{sp}}'^{\gamma_{\mathrm{sp}} - \gamma} r_0^{\gamma} \left(R_0^{3-\gamma_{\mathrm{sp}}} - R_{\mathrm{min}}^{3-\gamma_{\mathrm{sp}}} \right)} \right)^{4-\gamma} .$$

  where $R'_{\mathrm{sp}} = \alpha_\gamma r_0 \left(M_{\mathrm{BH}} / r_0^3 \right)^{\frac{1}{3-\gamma}}$.

- This criteria yields masses of the dark matter halo compatible with universal relations between black hole-galaxy masses
- For NFW-like profiles with $\gamma \neq 1$, we solve numerically $\int_{4R_S}^{R_{\mathrm{halo}}} 4\pi r^2 \rho(r) dr \lesssim M_{\mathrm{DM}}$ where $R_{\mathrm{halo}} = 5 \times r_0$

γ_{sp} from dimensional arguments

Assume a model consisting entirely of circular orbits. Assume that the density cusp is $\rho \sim r^{-\gamma}$ before the addition of the BH and $\rho \sim r^{-\gamma_{\rm sp}}$ after. Conservation of mass implies that

$$\rho_i r_i^2 dr_i = \rho_f r_f^2 dr_f \quad \Longrightarrow \quad r_i^{3-\gamma} \sim r_f^{3-\gamma_{\rm sp}}.$$

Conservation of angular momentum implies that

$$r_i M_i(r) = r_f M_f(r) \simeq r_f M_{BH} \quad \Longrightarrow \quad r_i^{4-\gamma} \sim r_f.$$

Combining these two results

$$\gamma_{\rm sp} = \frac{9-2\gamma}{4-\gamma}$$

Capture condition

- The spike vanishes at the radius of the unstable circular orbit for a marginally bound particle, $E = 1$ and $L_c = 4Gm$ (relativistic energy and angular momentum per unit mass). GS assumed $L_c = 8GM$
- The critical values of L and E are determined by the schwarzschild effective potential $dV(r)/dr = 0$.

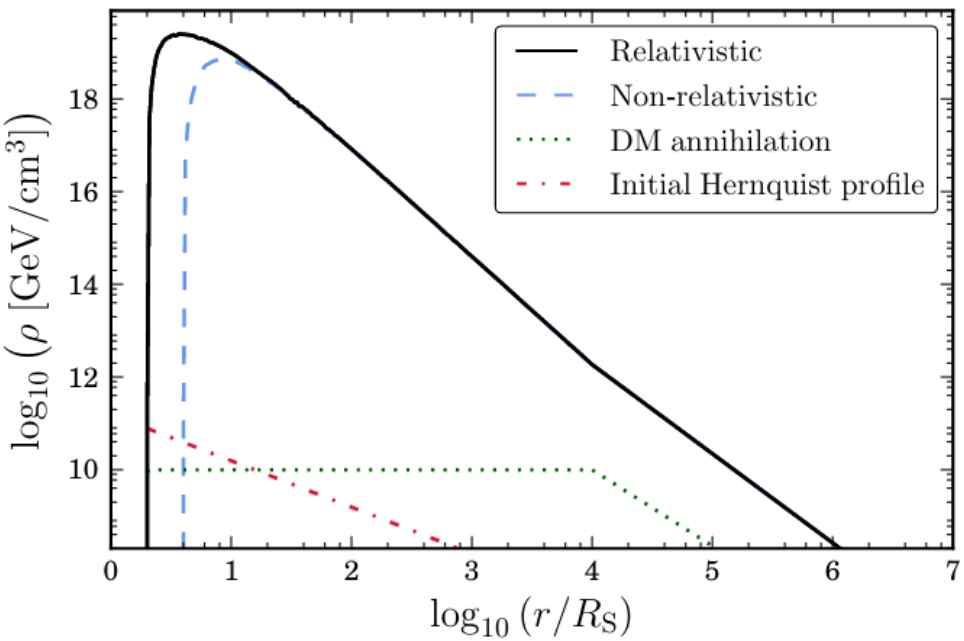

Coefficient C

For NGC 1068, the proton luminosity is

$$10^{43}\text{ergs}^{-1} \lesssim L_p \lesssim L_X \lesssim 10^{44}\text{ergs}^{-1} \rightarrow C \sim 0.1 - 1.$$

For TXS 0506 + 056, the proton luminosity in the single-zone model already violates the Eddington luminosity L_{Edd} , so our choice is conservative. Similarly for electrons $L_e \sim 8 \times 10^{47}\text{ergs}^{-1} \sim 20 L_{\text{Edd}}$

In principle, if the CR acceleration mechanism is understood, spectral modification due to BSM cooling may allow us to improve constraints and $C \sim 1$ is possible. For proton energies of interest, because neutrinos carry $\sim 5\%$ of the proton energy, we use $10 - 300$TeV for NGC 1068 and $2 - 20$PeV

For electrons, we use 50GeV – 2TeV

Eddington limit

- Maximum luminosity an AGN can achieve when there is balance between the force of radiation acting outward and the gravitational force acting inward. The state of balance is called hydrostatic equilibrium. When an AGN exceeds the Eddington luminosity, it will initiate a very intense radiation-driven stellar wind from its outer layers.

$$L_{\mathrm{Edd}} = \frac{4\pi G M m_{\mathrm{p}} c}{\sigma_{\mathrm{T}}}$$

$$-\frac{\nabla p}{\rho} = \frac{\kappa}{c} F_{\mathrm{rad}}$$

Electromagnetic emission from TXS 0506+056

IceCube, Fermi-LAT, MAGIC, AGILE, ASAS-SN, HAWC, H.E.S.S, INTEGRAL, Kanata, Kiso, Kapteyn, Liverpool telescope, Subaru, Swift/NuSTAR, VERITAS, and VLA/17B-403 teams, 18'

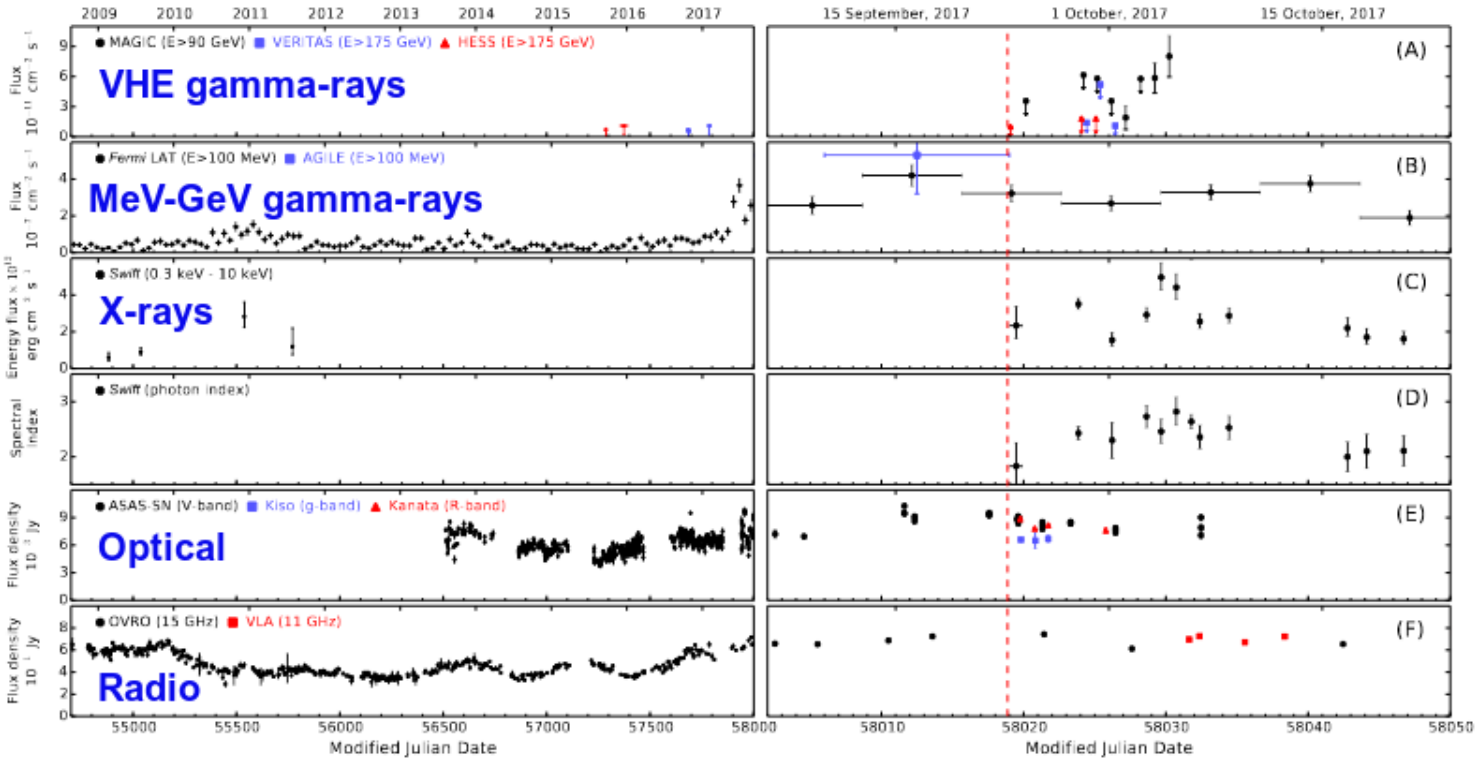

- Multi-wavelength photon observations show an excess compatible with IC-170922A.
- Chance coincidence between the neutrino and gamma-ray events is rejected at 3σ.

High-energy neutrino and gamma-ray production

- Hadronic models: Protons interact with ambient photons, producing neutral and charged pions decaying into both photons and neutrinos.
- Leptonic models: Low-energy photons arising from synchrotron radiation of accelerated electrons, and high-energy photons from inverse compton scattering of electrons with ambient photons.

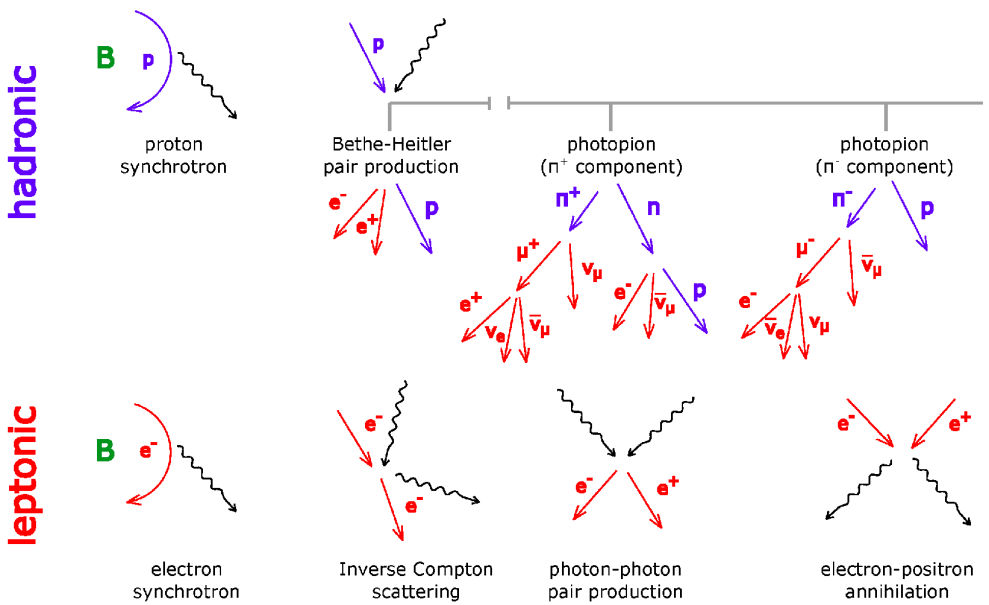

Gao, Fedynitch, Winter, Pohl, 19'

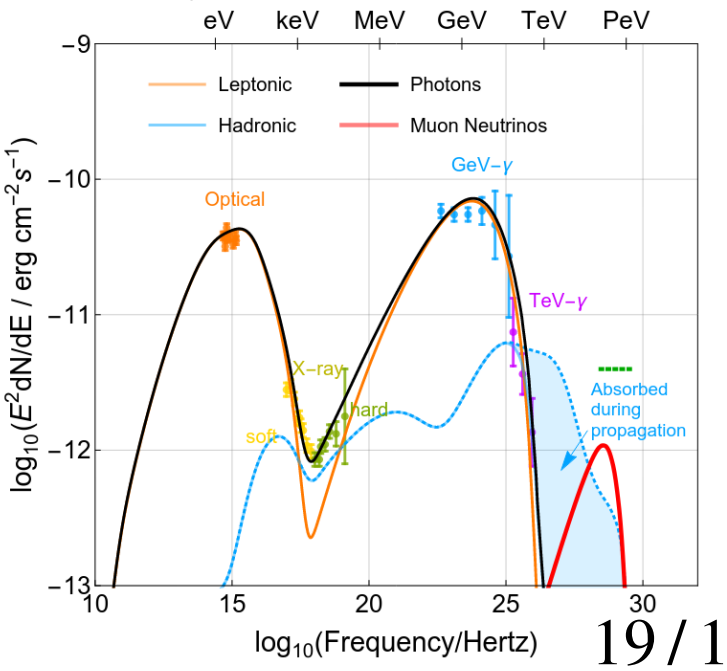

Extragalactic ν sources: TXS 0506+056 and NGC 1068

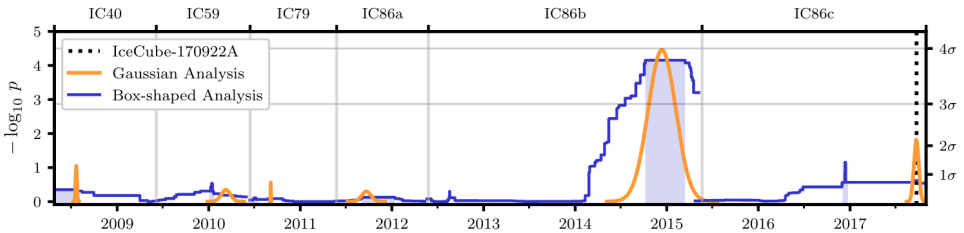

IceCube, 18' , 22'

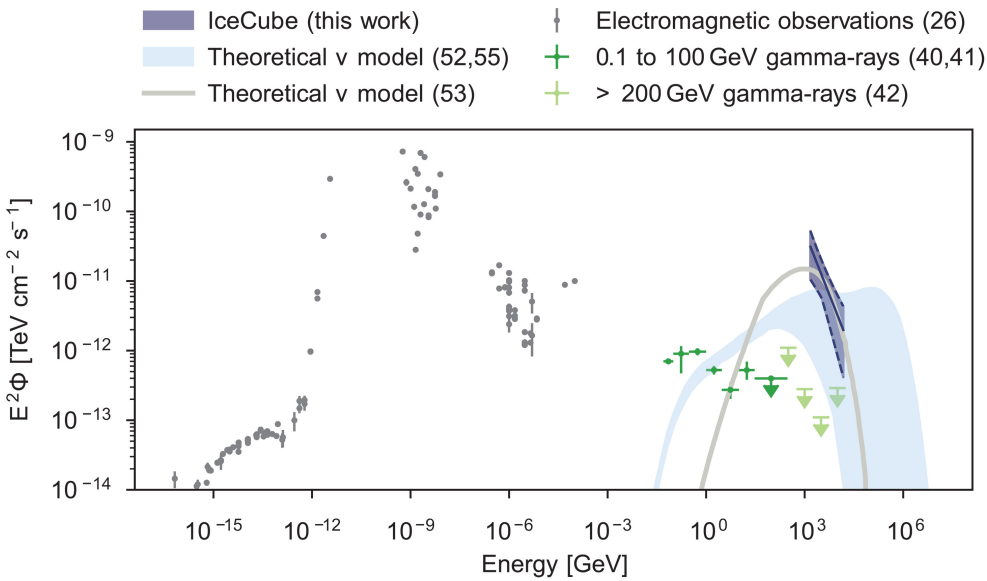

- IC-170922A: A ~ 290 TeV muon neutrino, identified with the blazar TXS 0506+056 in flaring state at origin direction.
- Subsequent analysis by IceCube with 9.5 years of data finds ~ 10 events above the atmospheric neutrino background, at 3.5 σ.
- IceCube observed ~ 80 neutrinos from the galaxy NGC 1068, at 4.2 σ.
- Electromagnetic emission from both sources was observed, but covering different wavelength ranges.

SED from NGC 1068 vs leptohadronic models

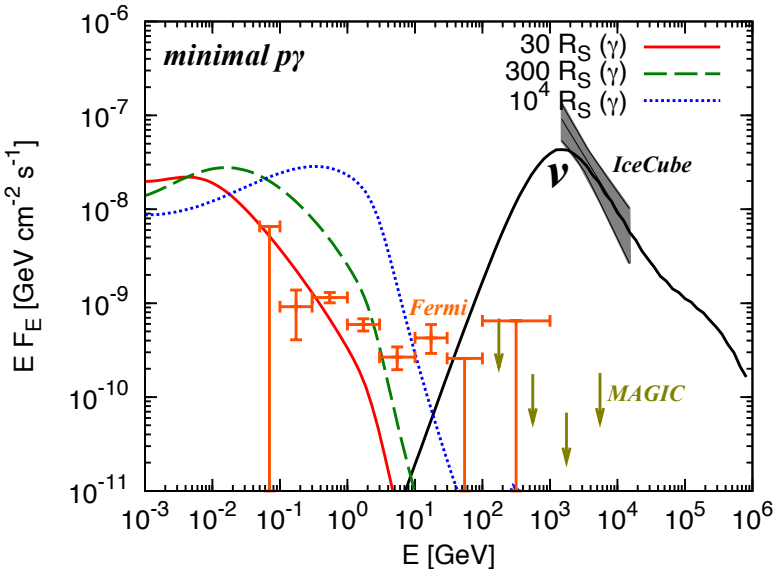

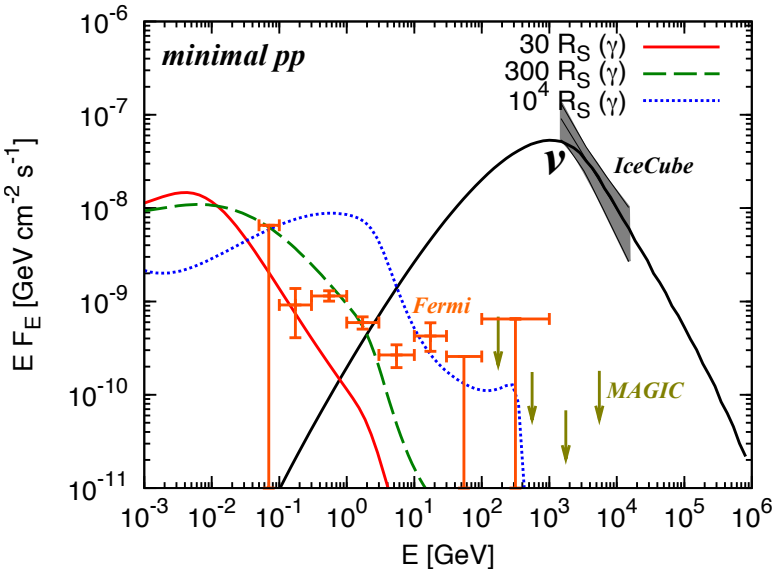

Murase, 22'

The cascade equation

The evolution of the neutrino and photon fluxes Φ_i due to scatterings can be described by a Boltzmann equation

$$\frac{d\Phi}{d\tau}(E_i) = -\sigma_{\mathrm{DM-i}}\Phi_i + \int_{E_\nu}^{\infty} dE_i' \frac{d\sigma}{dE_i}(E_i' \to E_i)\Phi(E_i')$$

with $\tau = \Sigma_{\mathrm{DM}}/m_{\mathrm{DM}}$, and the second term capturing the effect of the neutrino/photon energy being redistributed.

- Our criteria assumes implicitely that $\frac{\Phi_{\mathrm{obs}}}{\Phi_{\mathrm{em}}} \leq 1$, and the second term can be neglected.
- This was considered in **Cline et al, 22'**, finding more aggressive results, also due to different choices of R_{em}.

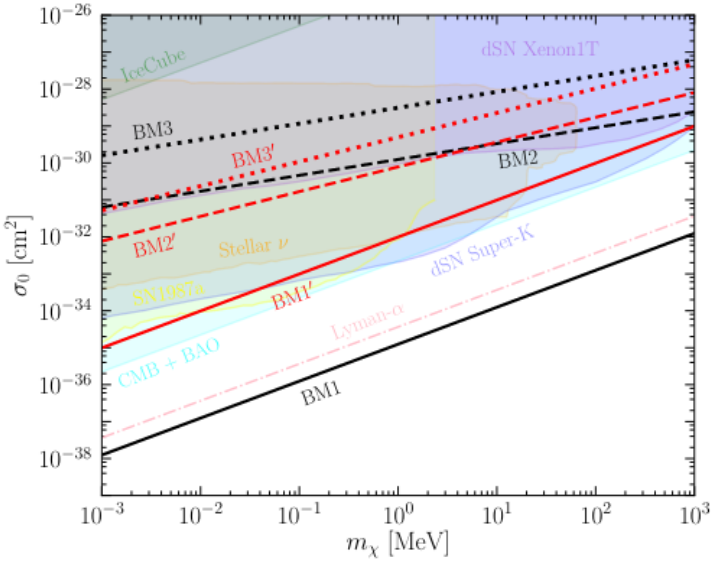

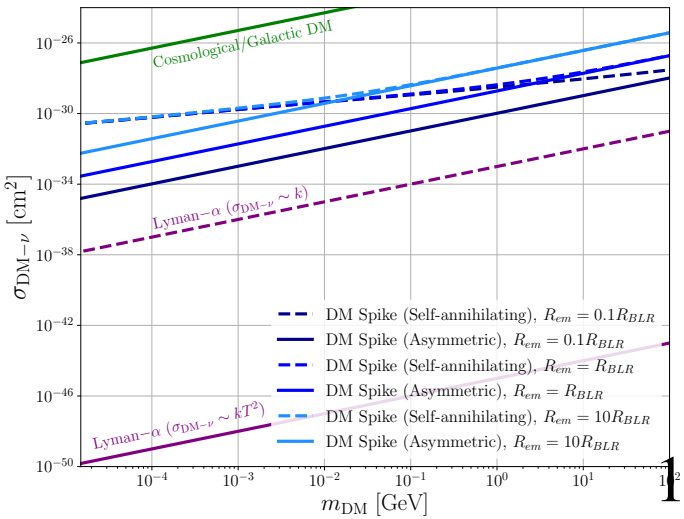

The cascade equation

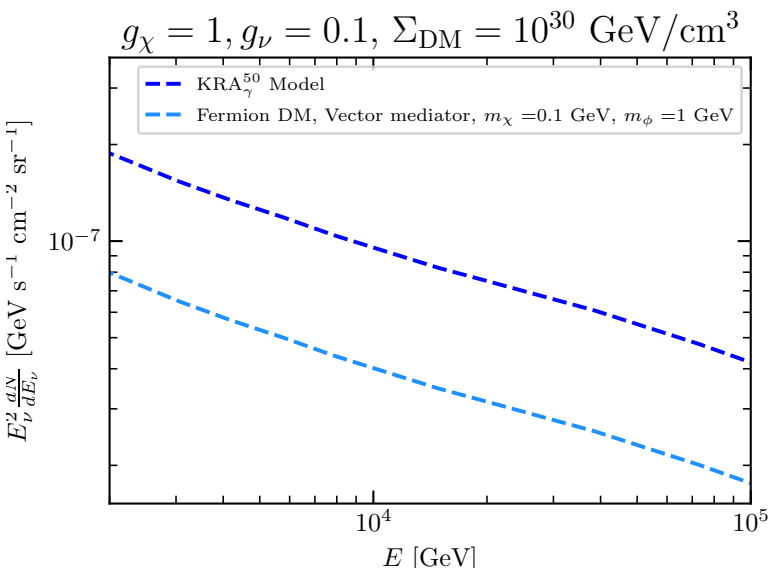

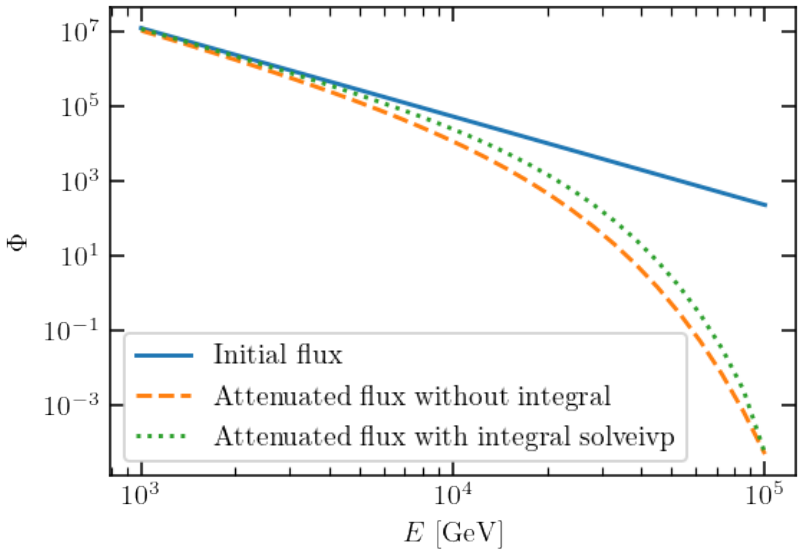

- If the DM-proton scattering cross section depends with the energy of the incoming neutrino, the second term of the cascade equation may contribute sizably in some instances.
- E.g when the dark matter-neutrino scattering proceeds via a Z' mediator, in the regime $m^2_{Z'} > m_\chi E_\nu$, the cross section rises linearly with the energy of the incoming neutrino.

Complementary constraints on the DM-ν cross section

- Complementary constraints (aside from cosmological ones) can be derived under the assumption that dark matter also couples to electrons with similar strength.
- However, these are model dependent

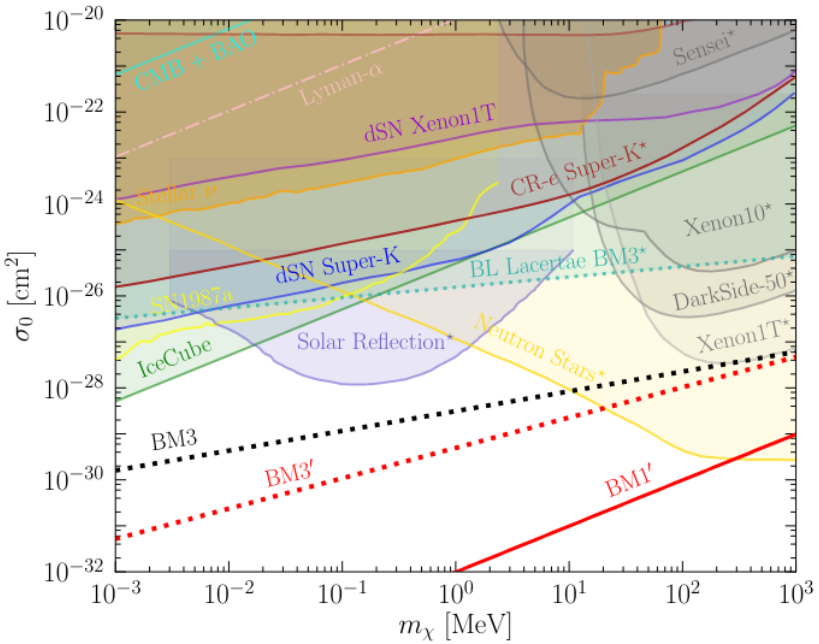

Models of the Spectral Energy Distribution (SED)

Gao, Fedynitch, Winter, Pohl, 19'

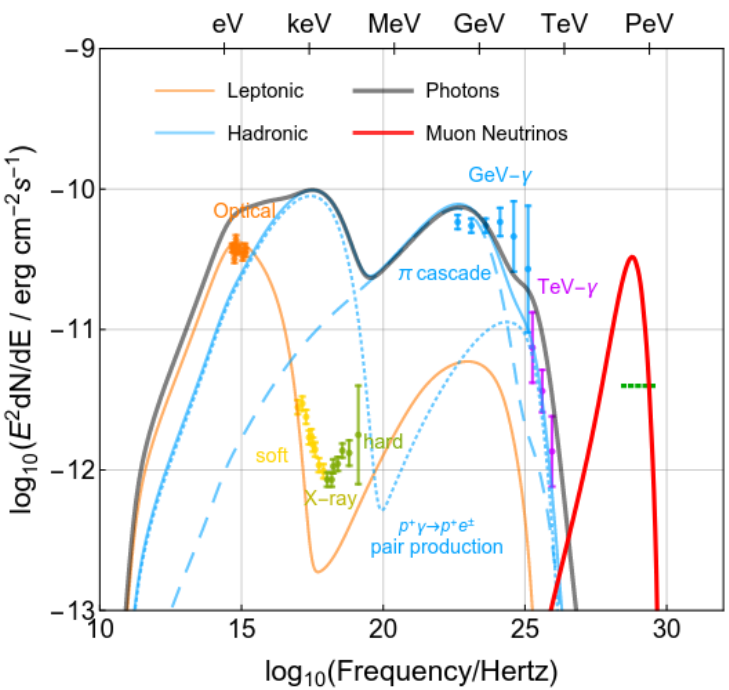

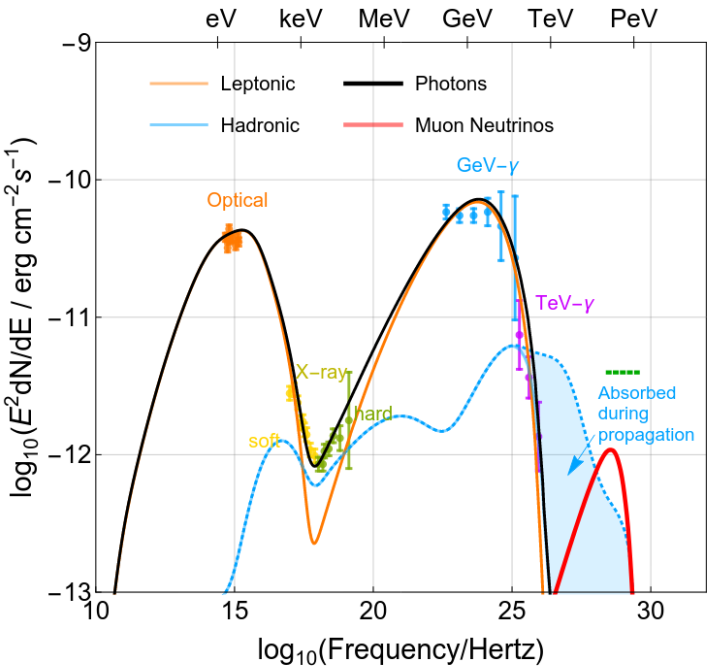

- Leptohadronic single-zone models are statistically compatible with the observed fluxes, although it predicts a significantly smaller neutrino flux than observed, otherwise it overshoots X-ray observations.
- Leptonic: First peak (synchroton radiation), second peak (Inverse Compton Scattering)
- Alternatives: Multi-zone and multi-epoch models (e.g **Xue, Liu et al, 19'**, **Petropoulou, Murase et al, 19'**)

Cosmological constraints

Dark matter interactions with neutrinos and photons suppress small-scales due to damped oscillations in the matter power spectrum.
MW satellite constraints are valid for $m_{\rm DM} \gg m_p$, since they assume

$$\sigma_{\gamma \rm DM} = \epsilon^2 \sigma_T \left(\frac{m_e}{m_{\rm DM}} \right)^2$$

Wilkinson, Boehm, Lesgourges, 14'

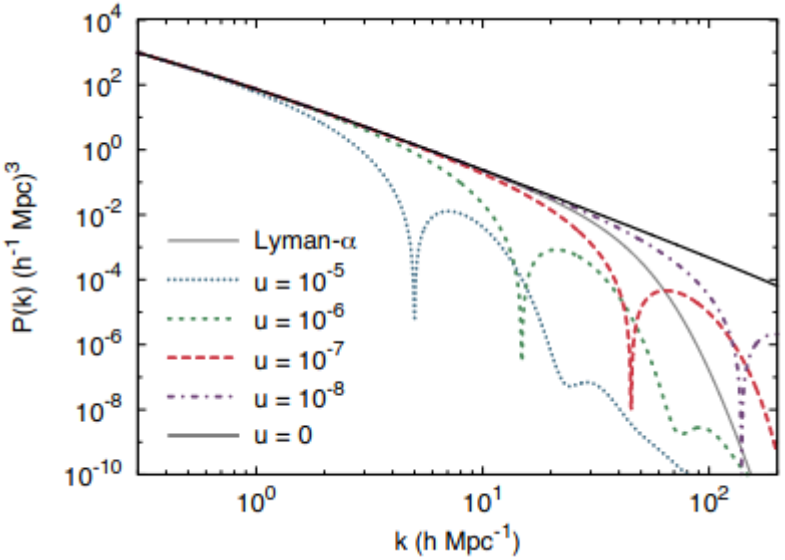

Wilkinson, Boehm, Lesgourges, 13'

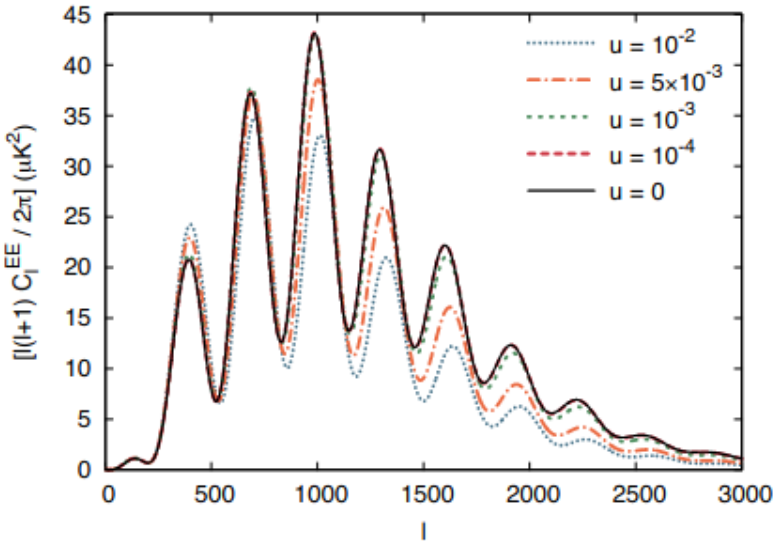

- The height of the peaks is changed due to collisional damping and delayed photon decoupling.

- The position of the peaks is shifted due to drag forces induced by the DM.

Constraints for values of the NFW slope γ

- The limits can vary 5 to 6 orders of magnitude
- For $\gamma = 0.6 - 1.4$, favoured by simulations, the limits only vary within one order of magnitude

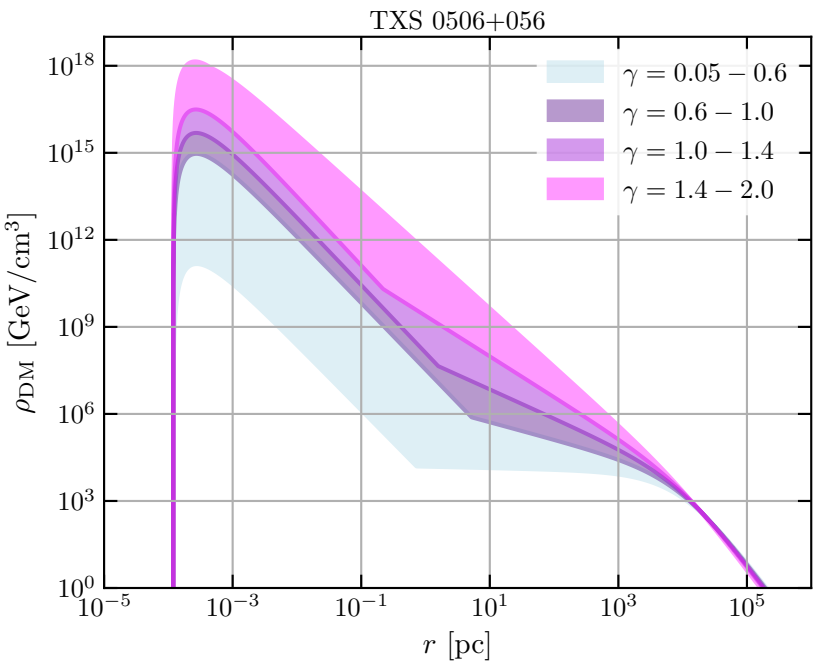

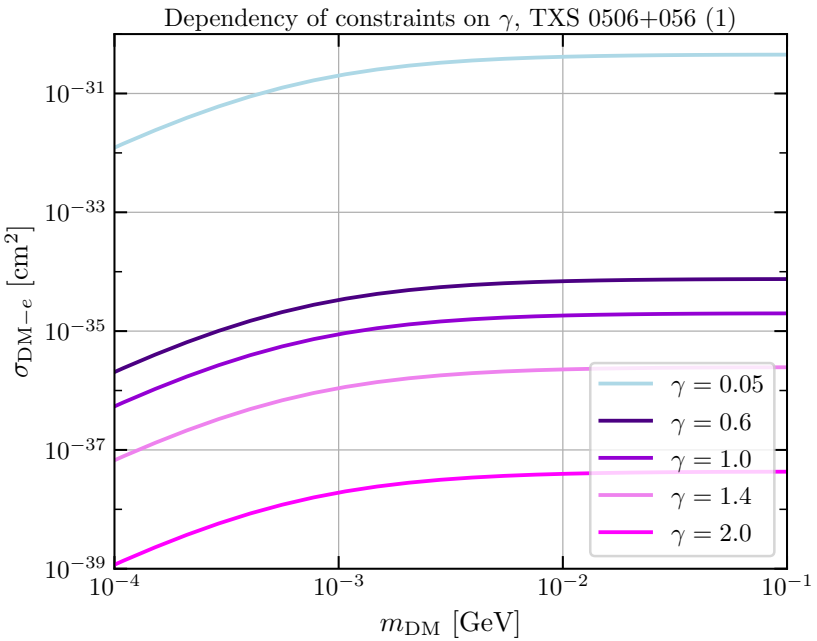

Constraints for shallower profiles

- Gravitational scattering of dark matter with stars may relax the spike to $\gamma_{\rm sp} = 1.5$.
- We assess this possibility when deriving upper limits on dark matter-neutrino scatterings from Tidal Disruption Events (TDE).

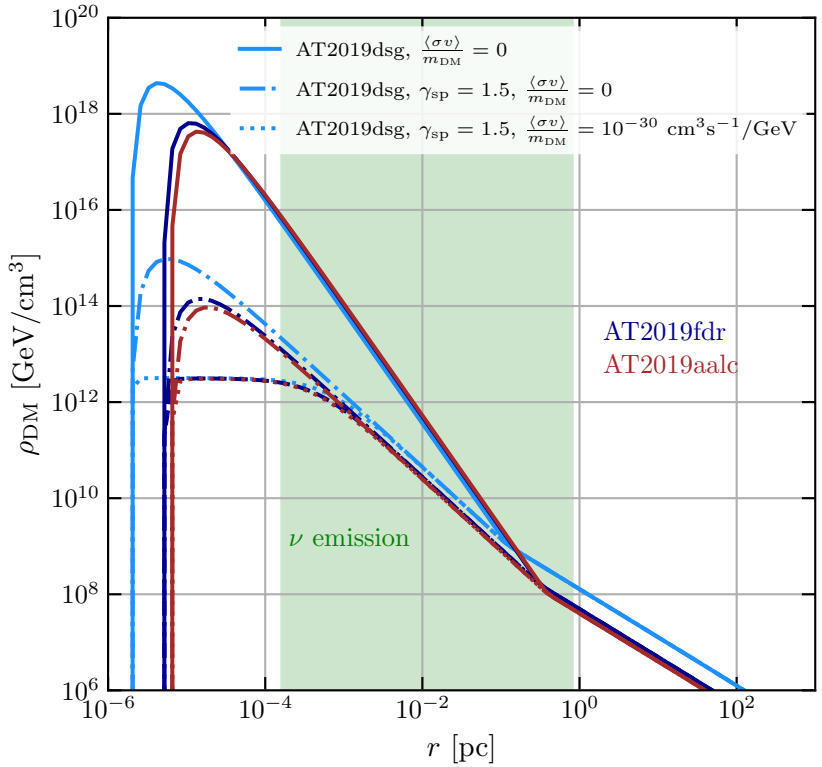

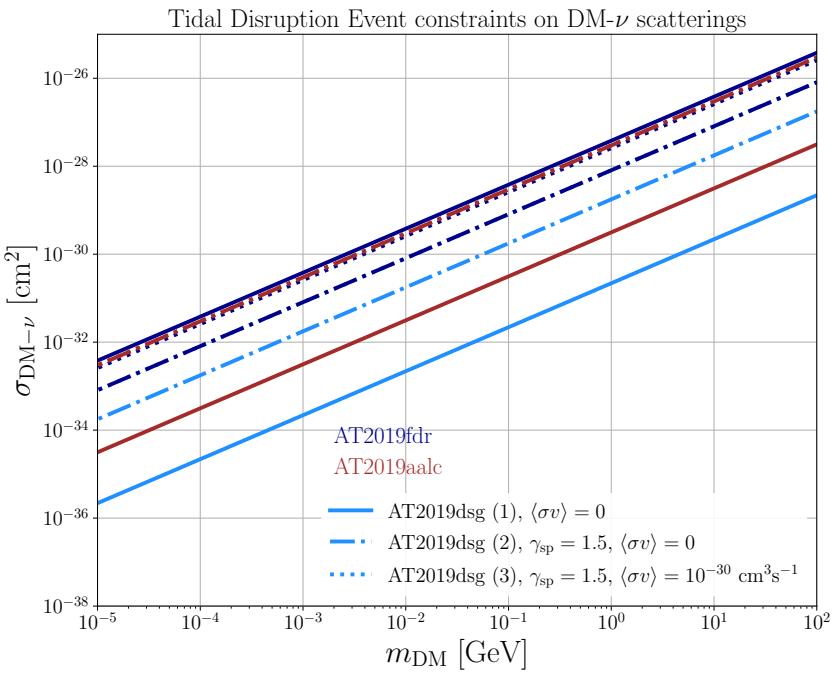

Simplified model considered for p, e bounds

We consider fermionic DM and a heavy scalar mediator

$$\mathcal{L}_{\phi,\chi} = g_\chi \phi \bar{\chi} \chi$$

and, e.g via Higgs-scalar mixing

$$\mathcal{L}_{\phi,\mathrm{SM}} = \phi \sin\theta \sum_f \frac{m_f}{v} \bar{f} f, g_f \equiv \frac{m_f}{v} \sin\theta,)$$

The differential scattering cross section is

$$\frac{d\sigma}{dT} = \frac{\sigma_{\mathrm{DM}-i}}{T_{\mathrm{DM}}^{\max}} \frac{F_i^2(q^2)}{16\,\mu_{\mathrm{DM}-i}^2\, s} (q^2 + 4m_i^2)(q^2 + 4m_{\mathrm{DM}}^2)$$

where $\sigma_{\mathrm{DM-i}}$ is the DM-proton or the dark matter-electron scattering cross section in the highly non-relativistic limit, i.e

$$\sigma_{\chi N}^{\mathrm{SI}}\left(q^2 = 0\right) = \frac{g_\chi^2 g_N^2 \mu_{\chi N}^2}{\pi m_S^4}$$

F_i is either the proton form factor or equal to one for electrons

$$F_p\left(q^2\right) = \left(\frac{1}{1+q^2/\Lambda^2}\right)^2 \quad \text{with} \quad \Lambda = 0.770\mathrm{GeV}$$

BBN constraints on light dark matter

- Light dark matter affects the expansion rate of the Universe, as well as the temperature of Standard Model particles, leaving signatures on primordial abundances and $N_{\rm eff}$

$$N_{\rm eff} = 3\left[\frac{11}{4}\left(\frac{T_\nu}{T_\gamma}\right)_0^3\right]^{4/3}\left(1+\frac{\Delta N_\nu}{3}\right)$$

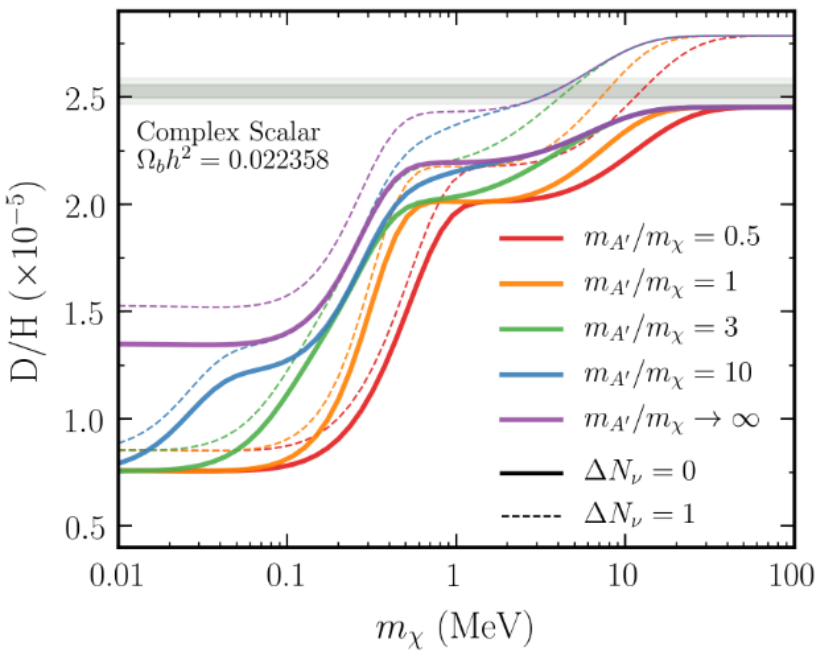

Giovanetti, Lisanti, Liu, Ruderman, 13'

NGC 1068 DM-photon scattering models

χ : Mediator

ψ: Dark matter fermion

$$\mathcal{L}_{\chi\psi} = g_{\chi\psi} \times \begin{cases} i\chi_{\bar{\psi}}\gamma_5\chi & \text{Pseudoscalar} \\ \chi\bar{\psi}\psi & \text{Scalar} \\ \chi_\mu\bar{\psi}\gamma^\mu\psi & \text{Vector} \end{cases}$$

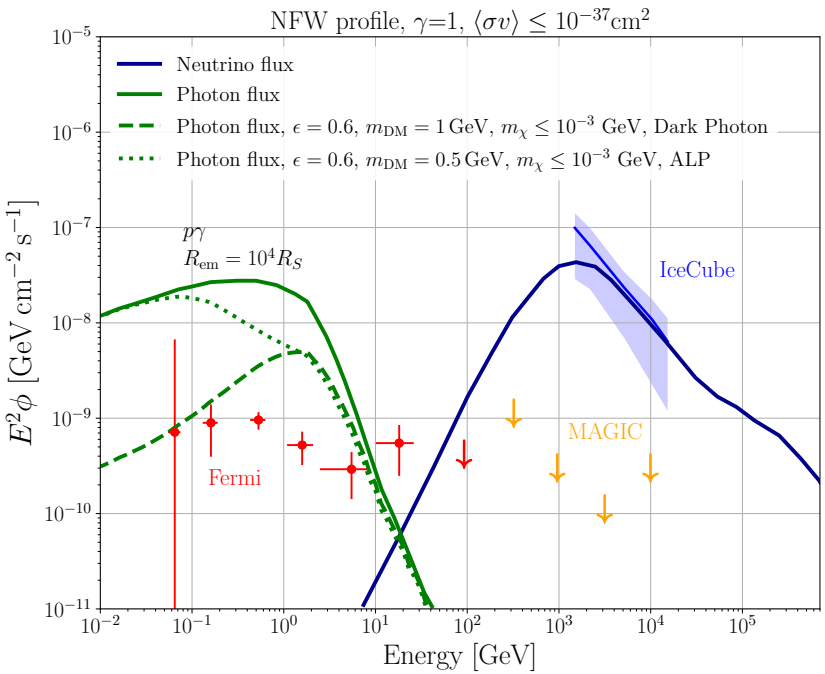
NFW profile, γ=1, $\langle\sigma v\rangle \leq 10^{-37}\mathrm{cm}^2$
Neutrino flux
Photon flux
Photon flux, $\epsilon = 0.6$, $m_{\mathrm{DM}} = 1\,\mathrm{GeV}$, $m_\chi \leq 10^{-3}$ GeV, Dark Photon
Photon flux, $\epsilon = 0.6$, $m_{\mathrm{DM}} = 0.5\,\mathrm{GeV}$, $m_\chi \leq 10^{-3}$ GeV, ALP
$p\gamma$
$R_{\mathrm{em}} = 10^4 R_S$
IceCube
MAGIC
Fermi
$E^2\phi$ [GeV cm^{-2} s^{-1}]
Energy [GeV]

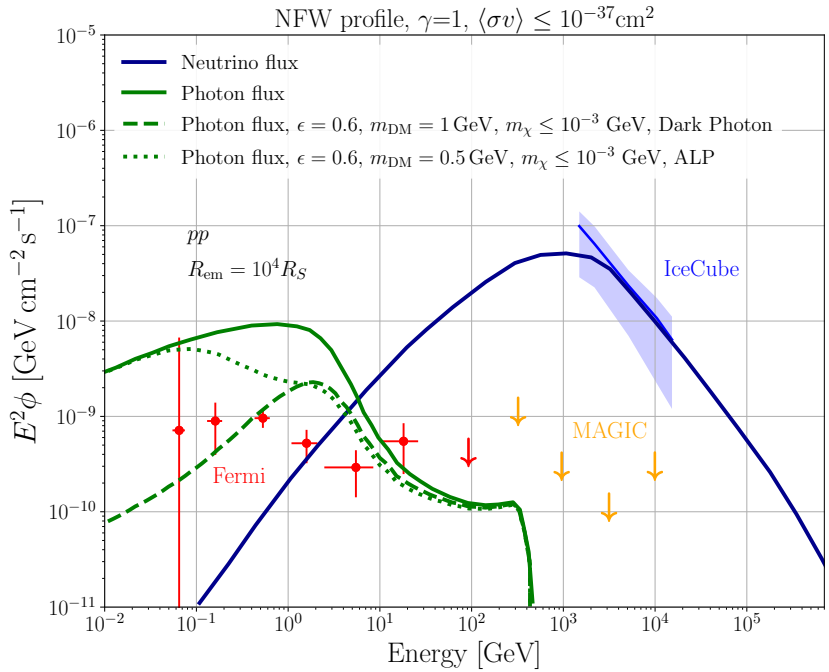
NFW profile, γ=1, $\langle\sigma v\rangle \leq 10^{-37}\mathrm{cm}^2$
Neutrino flux
Photon flux
Photon flux, $\epsilon = 0.6$, $m_{\mathrm{DM}} = 1\,\mathrm{GeV}$, $m_\chi \leq 10^{-3}$ GeV, Dark Photon
Photon flux, $\epsilon = 0.6$, $m_{\mathrm{DM}} = 0.5\,\mathrm{GeV}$, $m_\chi \leq 10^{-3}$ GeV, ALP
pp
$R_{\mathrm{em}} = 10^4 R_S$
IceCube
MAGIC
Fermi
$E^2\phi$ [GeV cm^{-2} s^{-1}]
Energy [GeV]

Dark matter halos

- In ΛCDM, dark matter halos form hierarchically from density perturbations in the initial density field
- Baryons cluster in the same way as CDM when perturbations on galaxy scales are still linear
- Eventually, baryonic gas can be shocked and heated, clustering towards the center more than CDM.

Dark matter halos

- Halos are spherical and virialized objects formed from regions with overdensities larger than a critical overdensity $\delta(x,t) > \delta_c$. Further assuming a gaussian distribution, the PS halo mass function reads:

  $$\frac{dn}{dM} = \sqrt{\frac{2}{\pi}} \frac{\bar{\rho}}{M} \frac{\delta_c}{\sigma^2} \frac{d\sigma}{dM} \exp\left[-\frac{\delta_c^2}{2\sigma^2}\right]$$

- N-body simulations yielded universal halo profiles

  $$\rho(r) = \rho_{\rm crit} \frac{\delta_{\rm char}}{(r/r_{\rm s})\,(1 + r/r_{\rm s})^2}$$

  where $r_{\rm s}$ is a scale radius, and $\delta_{\rm char}$ is a characteristic overdensity. The NFW profile changes gradually from having a -1 slope near the center to -3 at large radii. Halos formed by hierarchical clustering seem to have a universal density profile with enclosed mass

  $$M(r) = 4\pi\bar{\rho}\delta_{\rm char}\, r_{\rm s}^3 \left[\ln(1 + cx) - \frac{cx}{1 + cx}\right]$$

  where $x \equiv r/r_{\rm h}$, and

  $$c \equiv \frac{r_{\rm h}}{r_{\rm s}}$$

  is the halo concentration parameter, and r_h is the bounding radius of a halo.

Dark matter halos

- Early ΛCDM simulations predicted cuspy dark matter halos scaling as $\rho \propto r^{-1}$ in the inner regions of the galaxy
- Current observational data suggests dark matter cores in the inner regions of galaxies, and simulations including baryonic physics are still inconclusive

Oh et al, 11'

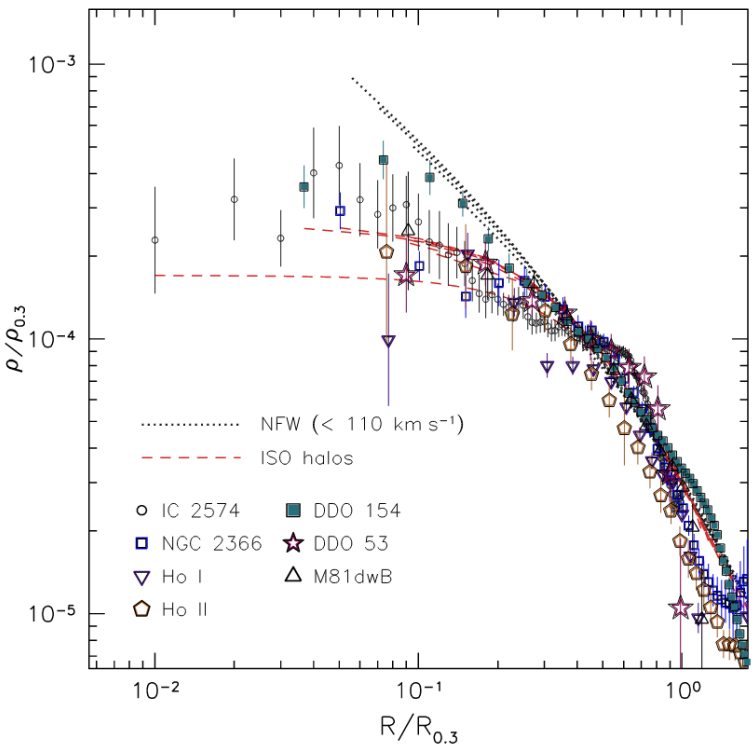

We adopt the generalized NFW profile

$$\rho(r) = \rho_0 \left(\frac{r}{r_0}\right)^{-\gamma} \left(1 + \frac{r}{r_0}\right)^{-3+\gamma}$$

with $\gamma \in [0, 2]$

Dark matter distribution in the local universe

Böhringer, Chon, Collins ’19

Karachentsev, Telikova ’18

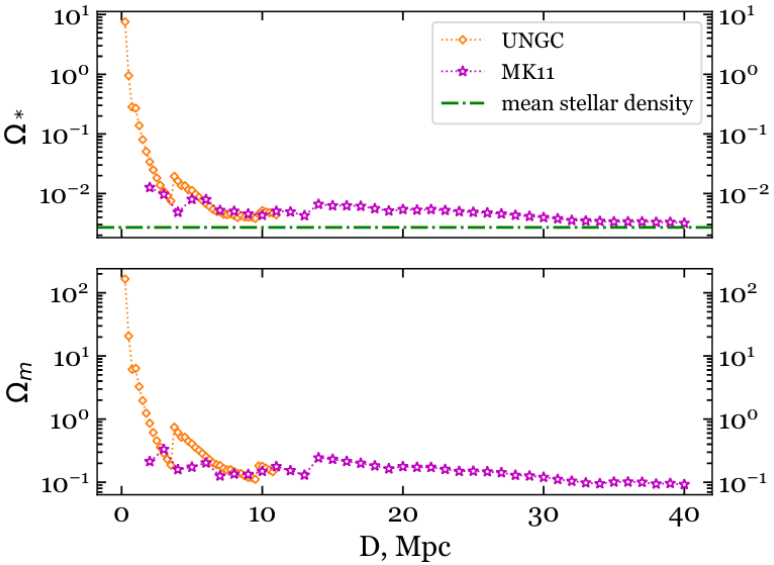

TABLE 2 Mean densities and total masses of the stellar and dark matter within spheres with radii D.

D Mpc	Sample	$M_*(< D)$ $M_\odot$	$\Omega_*(< D)$ %	$M_{tot}(< D)$ $M_\odot$	$\Omega_m(< D)$
11	UNGC (LV)	2.7×10^{12}	0.44	1.0×10^{14}	0.17
11	MK11	3.0×10^{12}	0.50	1.1×10^{14}	0.18
11	KT17,lum	2.3×10^{12}	0.39 ± 0.11	1.1×10^{14}	0.18 ± 0.05
	KT17, dyn			1.9×10^{14}	0.31 ± 0.17
40	MK11	9.2×10^{13}	0.32	2.7×10^{15}	0.09 ± 0.03
40	KT17, lum	7.1×10^{13}	0.24 ± 0.08	4.0×10^{15}	0.14 ± 0.06
	KT17, dyn			3.5×10^{15}	0.12 ± 0.08
135	T15b, lym	2.5×10^{15}	0.22 ± 0.02	1.8×10^{17}	0.16 ± 0.01
	T15b, dyn			0.6×10^{17}	0.05 ± 0.002

- Observational measurements of the average DM density $\Omega_m \approx 0.09 - 0.18$ are systematically lower than the cosmic value $\Omega_m = 0.31$
- The discrepancy might point towards a significant fraction of the DM being distributed homogeneously within clusters of galaxies.
- We are lacking simulations of the dark matter distribution in the Local Universe, but dedicated studies are on the way (e.g CLUES, Hestia).

Dark matter spike formation

Adiabatic growth: A substantial increase in $M_{\rm BH}$ takes place after its initial formation, and the mass is acretted slowly to the pre-existing seed. Mathematically:

Peebles, 72'
Quinlan, Hernquist, Sigurdsson, 95'

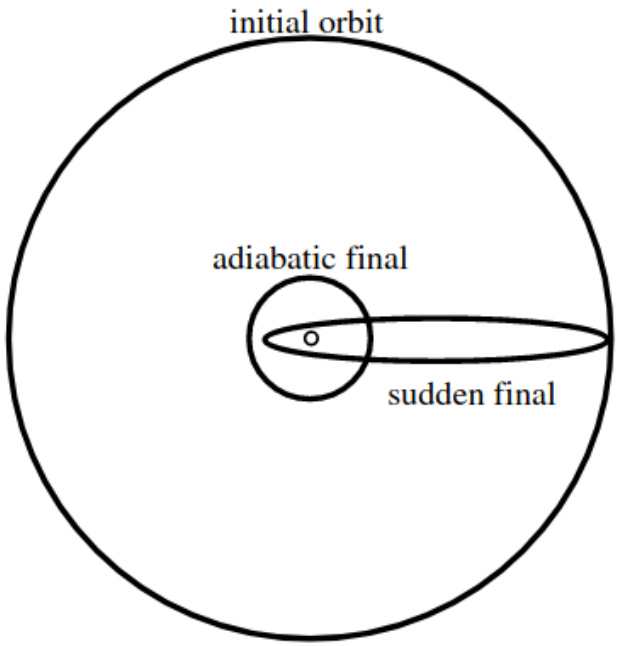

$$\rho'(r) = \int_{E_{m'}}^{0} dE' \int_{L'_c}^{L'_m} dL' \frac{4\pi L'}{r^2 v_r} f'(E', L')$$

$$v_r = [2(E' + \frac{GM}{r} - \frac{L'}{2r^2})]^{1/2}$$

$$E'_m = -\frac{GM}{r}(1 - \frac{4R_S}{R})$$

$$L'_c = 2cR_S,\ L'_m = [2r^2(E' + \frac{GM}{r})]^{1/2}$$

Adiabatic conditions :

$$f'(E', L') = f(E, L) \rightarrow \text{Phase-space distribution conservation}$$

$$L' = L \rightarrow \text{Angular momentum conservation}$$

$$I'(E', L') = I(E, L) \rightarrow \text{Radial action conservation}$$

The dark matter spike profile

The dark matter in the vicinity of a black hole that grows adiabatically forms a dense spike with profile:

Gondolo, Silk, 99'

$$\rho_{\rm sp}(r) = \rho_R \, g_\gamma(r) \left(\frac{R_{sp}}{r}\right)^{\gamma_{\rm sp}} , \partial\rho/\partial t = -\sigma v \rho^2/m$$

- $R_{\rm sp} = \alpha_\gamma r_0 (M_{\rm BH}/(\rho_0 r_0^3)^{\frac{1}{3-\gamma}}$ $\longrightarrow$ Size of the spike
- $r_0 \longrightarrow$ Scale radius of the host galaxy
- $g_\gamma(r) \simeq (1 - \frac{4R_S}{r}) \longrightarrow$ Captured particles by the BH
- $\gamma_{\rm sp} = \frac{9-2\gamma}{4-\gamma} \longrightarrow$ Cuspiness of the spike ($\gamma = 1$ for an NFW profile)
- $\rho_R = \rho_0 \left(R_{\rm sp}/r_0\right)^{-\gamma}$, and ρ_0 is a normalization used to match the outer profile, and to reproduce the total mass of the galaxy

Only valid for $r \leq R_{\rm sp}$, and in scenarios where the dark matter does not self-annihilate (e.g asymmetric dark matter or axions).

Acceleration mechanisms in AGN

- 2 order Fermi acceleration: Clouds of ionized gas in the interstellar medium are moving w.r.t to the galactic frame, reflecting charged particles passing through them. Energy gain derived by double change of reference:

$$\left\langle \frac{\Delta E}{E} \right\rangle = \frac{\beta^2 + \beta^2/3}{1-\beta^2} \simeq \frac{4\beta^2}{3} \tag{1}$$

- 1st order Fermi acceleration (diffusive shock acceleration): Energy gain after a charged particle has undergone a cycle upstream $\rightarrow$ downstream $\rightarrow$ upstream. Difference steams from shock velocity smaller than charged particle velocity $v \simeq c \gg v_{\rm sh}$

$$\left\langle \frac{\Delta E}{E} \right\rangle = \frac{4}{3}\beta \tag{2}$$

- Demanding that the Larmor radius of the particle, $R_L = \varepsilon/(qB)$, does not exceed the size of the acceleration region, the maximum particle energy after escaping the accelerator:

$$\varepsilon_{\rm max} = qB\mathcal{R}, \tag{3}$$

Acceleration mechanisms in AGN

- $L_\gamma \sim L_\gamma$, and energies of ambient photon field and density can be measured ϵ, so the neutrino-gamma-ray connection can be reconstructed to some extent, and the energies of initial protons and electrons can be inferred. $E_{\rm th} = \frac{2m_p m_\pi + m_\pi^2}{4\epsilon} \simeq 7 \times 10^{16} \left(\frac{\epsilon}{\rm eV}\right)^{-1}$ eV
- Acceleration can happen in the coronae, via shocks formed from magnetic recconection, but also from shear and turbulence in the jet.

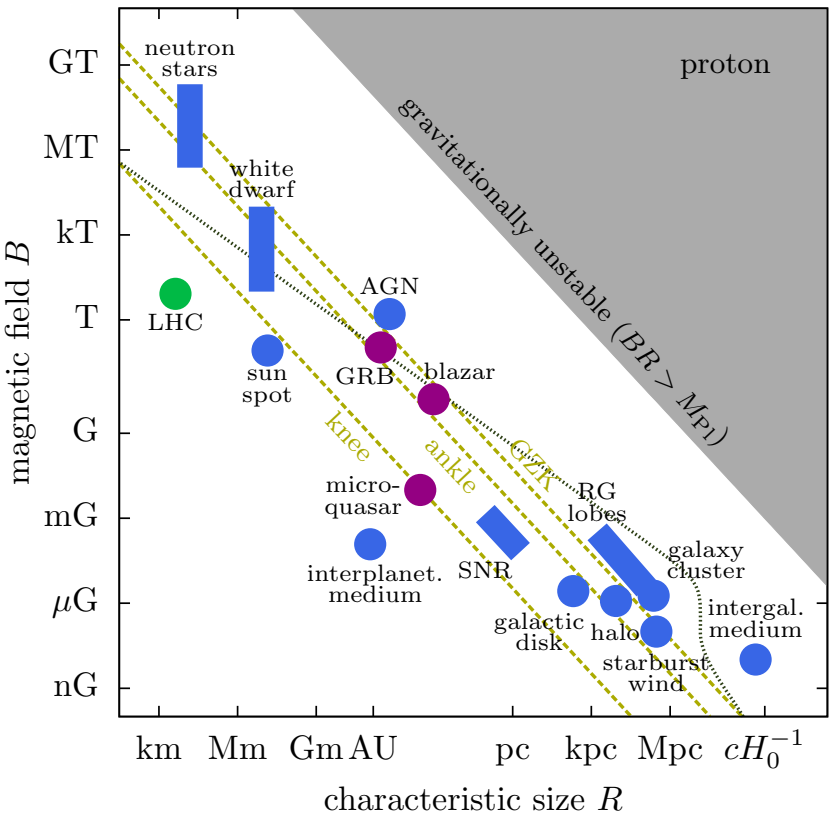

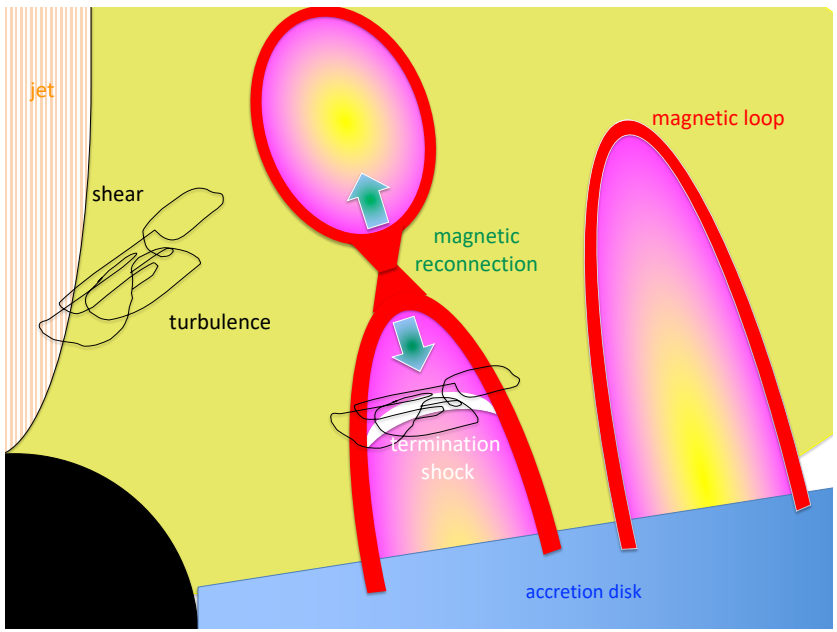

Astrophysical evidence for dark matter

Coma cluster observations: $M \simeq 1.6 \times 10^{14} M_\odot$. Using the virial theorem, the average kinetic energy and potential energy in a system are related via

$$2\langle T \rangle + \langle U_{\text{tot}} \rangle = 0 \tag{4}$$

where the potential energy is

$$|U| = \frac{GM^2}{R} \tag{5}$$

and the kinetic energy is

$$T = \frac{1}{2} M \left\langle v^2 \right\rangle = \frac{3}{2} M \left\langle v_\parallel^2 \right\rangle \tag{6}$$

where $v_\parallel$ is the tangential velocity of galaxies. For the measured values of the velocities of galaxies in the Coma cluster, Zwicky found

$$M \simeq 1.9 \times 10^{15} M_\odot \tag{7}$$

which is ~ 10 larger than visible matter.

Astrophysical evidence for dark matter

$$\frac{GM(r)m}{r^2} = \frac{mv_{rot}^2}{r}, M(r) = \int_0^r 4\pi\rho(r')r'^2 dr' \tag{8}$$

$$v_{rot} = \sqrt{\frac{GM(r)}{r}}, \tag{9}$$

In the center of the galaxy the density is roughly constant and $v_{rot} \propto r$. This can only approximate the observed rotation curve at the very core of the galaxy. In the outskirts, $M(r)$ is constant, and $v_{rot} \propto r^{-1/2}$.

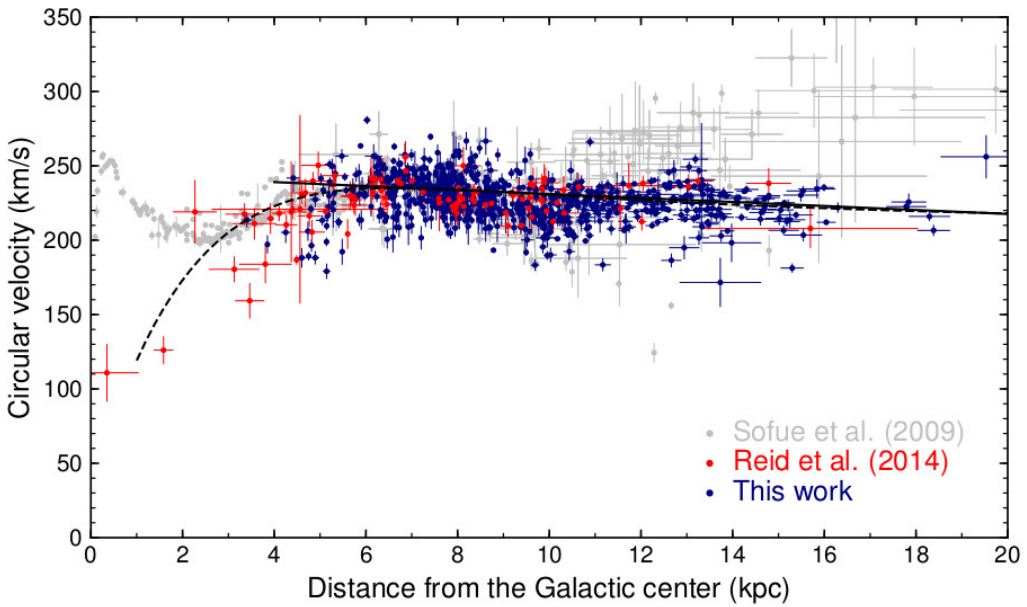

Astrophysical evidence for dark matter

In GR, a point mass deflects light ray with impact parameter b by an angle approximately equal to

$$\hat{\alpha} = \frac{4GM}{c^2 b} \tag{10}$$

- Strong gravitational lensing → Deflection angle can be measured, e.g from clusters of galaxies
- Systematic alignment of background sources around the lensing mass of 0.1 – 1%
- Colliding galaxy clusters → allows to compare electromagnetic map with gravitational lensing map

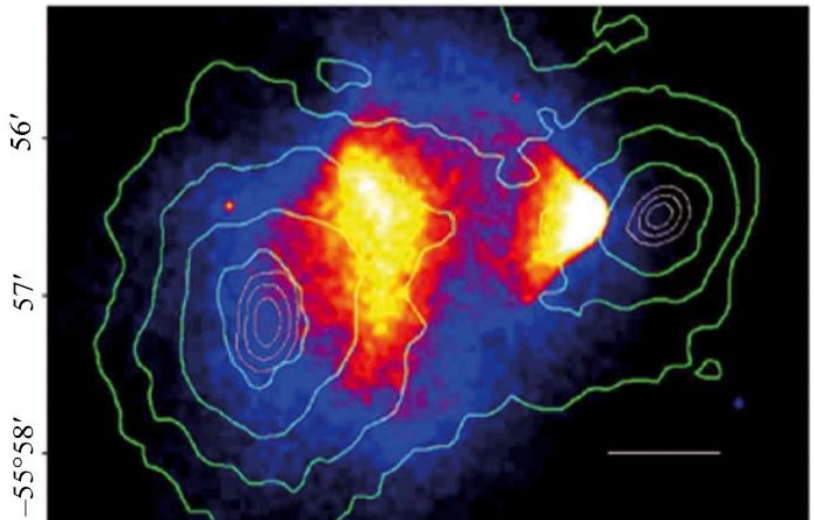

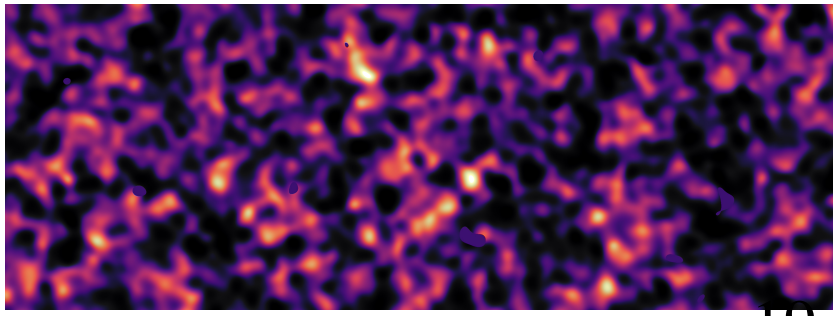

Astrophysical evidence for dark matter

Dark matter-free galaxies also provide evidence for dark matter w.r.t MOND theories. Violent processes can disrupt the dark matter content of a galaxy, while MOND should be present anywhere.

- For a MOND acceleration scale of $a_0 = 3.7 \times 10^3$ km^2 s^2 kpc^1 the velocity dispersion of NGC1052–DF2 is $\sigma \sim (0.05 G M_* a_0)^{1/4} \sim 20$ km s^{-1}, two times larger than the upper limit.

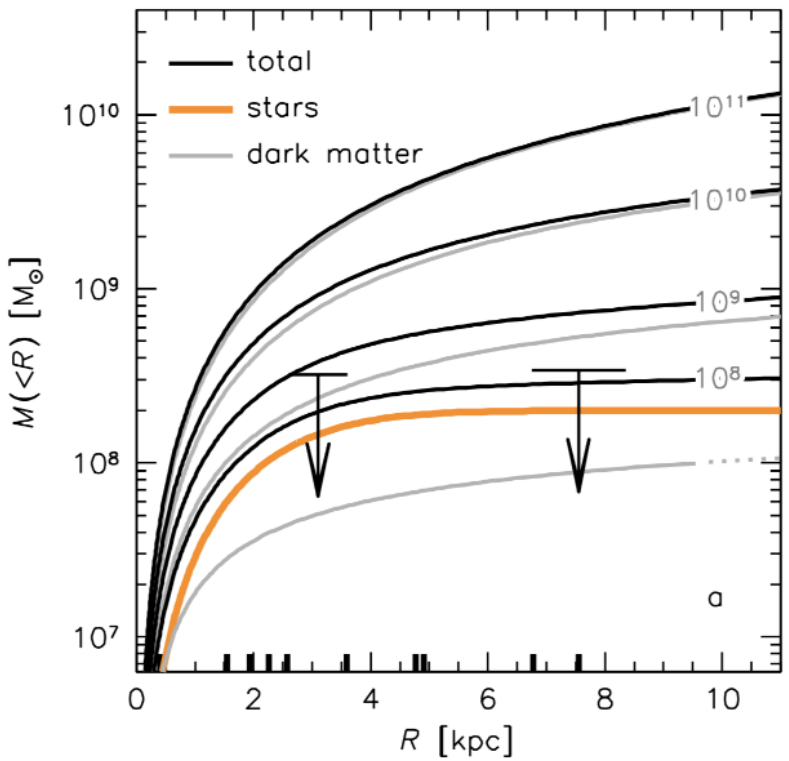

Cosmological evidence for dark matter

- CMB: Since the coupling of DM and baryons to photons is different, the power spectra of temperature and polarization fluctuations of recombination epoch photons depends crucially on the ratio between both components.
- BBN: Formation of light elements like deuterium is sensitive to the baryon density at the time → indirect limit on dark matter density when combined with CMB

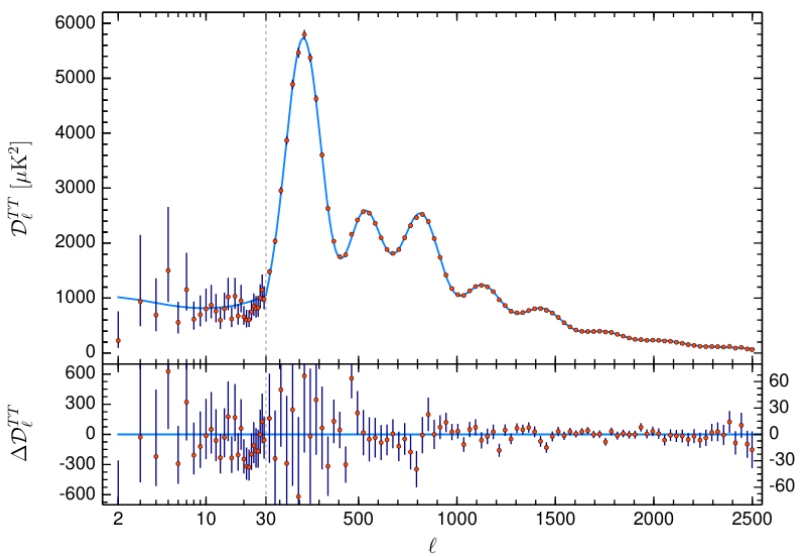

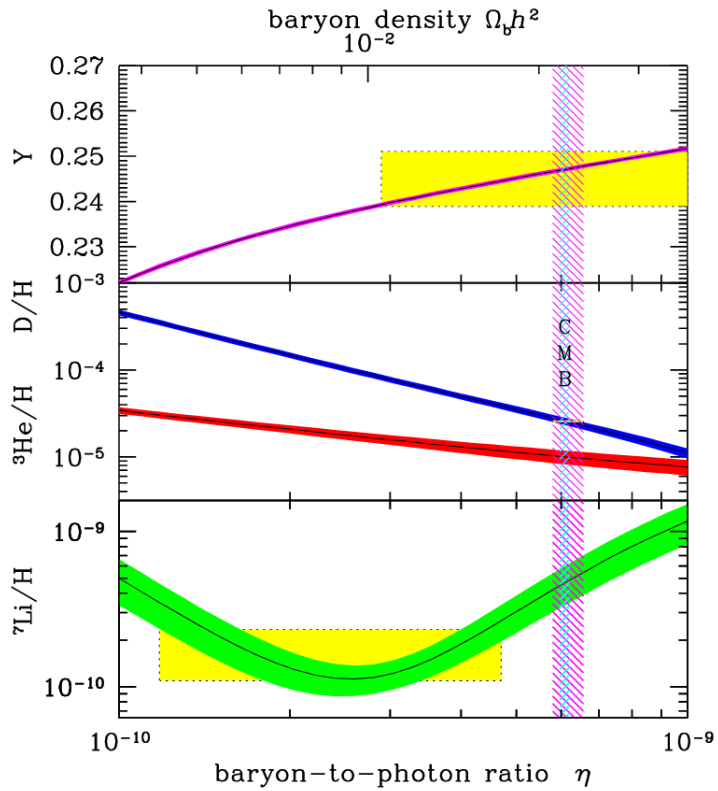

Cosmological evidence for dark matter

- BAO: On larger scales, systematic distortions less than $\sim 1\%$ in the BAO positions between the galaxies and the linear matter distribution $\rightarrow$ confirmed with redshift surveys
- Ly-α forest: The pattern of absorption lines from the Lyman-α transition of neutral hydrogen in the spectrum of distant quasars also provide info on the distribution on the large scale structure of the Universe, consistent with ΛCDM